A Reprint from the

PROCEEDINGS

Of SPIE-The International Society for Optical Engineering

Volume 619

Cryogenic Optical Systems and Instruments II

23–24 January 1986
Los Angeles, California

Cryogenic star-tracking telescope for Gravity Probe-B

C. W. F. Everitt
Stanford University
Relativity Gyroscope Program, Hansen Laboratories
Stanford University, Stanford, California 94305

D. E. Davidson
Optical Instrument Design Company

R. A. Van Patten
Stanford University
Relativity Gyroscope Program, Hansen Laboratories
Stanford University, Stanford, California 94305

Cryogenic star-tracking telescope for Gravity Probe B

C.W.F. Everitt
Stanford University

D.E. Davidson
Optical Instrument Design Company

R.A. Van Patten
Stanford University

Relativity Gyroscope Program, Hansen Laboratories,
Stanford University, Stanford, California 94305

Abstract

This paper describes the design, development and preliminary testing of the cryogenic star-tracking telescope used as an optical reference for the gyroscopes in the Gravity Probe B Relativity Gyroscope experiment. The telescope is operated at 1.8 K; it is fabricated entirely from fused quartz components held together by optical contacting; it has a physical length of 14 in, a focal length of 150 in and an aperture of 5.6 in. Readout is by two photomultiplier chopper-detector assemblies at ambient satellite temperature. When fully operational the telescope may be expected to have a precision approaching 0.1 marc-s over a linear range of ±70 marc-s. Its projected noise performance corresponds to an angular resolution of 1 marc-s in 1 Hz bandwidth. The paper includes a theoretical analysis, a description of the design and fabrication of a laboratory version of the telescope, a discussion of techniques of optical contacting, an account of vibration tests on a separate mass model of the telescope, a description of the artificial star developed for optical tests, and an account of preliminary experimental results.

History and background considerations

The Gravity Probe B Relativity Gyroscope experiment requires an exceedingly precise star-tracking telescope to serve as a reference between the gyroscopes and the guide star Rigel. Since the goal of the experiment is to measure certain relativity effects to better than 1 marc-s/yr, the telescope must have a resolution surpassing 1 marc-s, and its development presents a variety of interesting challenges.

Before going into details we emphasize that the question of telescope design cannot be treated in isolation. Although the final design appears simple it took several years to establish. Arriving at it required an investigation of a wide range of systems issues, such as the configuration of the gyroscopes, the design of the spacecraft pointing controller, the provision of a means for extracting relativity signals from the data, and so forth. In this introductory section of the paper we summarize a few broad considerations. The next two sections provide a description of the telescope design and a qualitative discussion of its rationale. Later sections contain a theoretical analysis, an account of fabrication procedures, a description of the artificial star for testing the telescope, and preliminary test results.

Our goal, as explained in the accompanying paper by Bardas et.al.,[1] is to determine to better than 1 marc-s/yr the relativistic precessions of a set of gyroscopes in earth orbit, measured with respect to the absolute inertial space provided by the framework of the fixed stars. In carrying out the measurements we choose to align the gyroscopes approximately with the line of sight to a particular guide star (Rigel) near the celestial equator, and also to roll the spacecraft continuously with 10 min period approximately about the same line. To execute a successful experiment four fundamental issues need to be addressed: (1) gyro drift performance, (2) gyro readout performance, (3) reference of the gyro signals (a) to Rigel (b) to a roll reference plane established by Rigel and another star roughly 90° away from it on the celestial sphere, (4) reference of Rigel to absolute inertial space. The four issues lead in turn to the nine fundamental requirements spelled out in papers by Everitt[2] and Young[3], to which should be added a tenth requirement on roll reference. Gyro readout and drift performance are discussed in the paper by Bardas et.al. A separate document by Anderson and Everitt[4] covers reference of the guide star to inertial space, i.e. determining the absolute proper motion of Rigel. Here we set telescope design in the context of the end-to-end task of referring the gyro spin axes to the line of sight to the guide star.

Notice that the role of the telescope in Gravity Probe B is purely intermediary. Our

interest is in referring the gyroscope to Rigel, not in measuring the orientation of the quartz block in which the gyroscopes are mounted. This consideration led Pugh[5] early on, and later independently Kaspar and Frisch[6], to propose schemes for experiments in which the optical system would form an integral part of the gyroscopic object, allowing the quantity of interest to be determined directly using a single readout device, instead of as in our experiment through the subtraction of gyroscope signals from telescope signals. Ingenious as their suggestions were, we prefer the less direct approach. To reach the ultimate in gyro drift performance one needs a spinning body of extreme roundness and homogeneity; attempts to incorporate the optics into the gyro rotor inevitably compromise this. Also, any such scheme leads to having a single very large gyroscope operated as a drag-free proof mass, losing one of the most attractive features of the present GP-B design - the ability to make cross-checks between four different gyroscopes operating under similar but not identical conditions. For these and other more technical reasons we favor having an independent telescope.

The telescope required is, of course, a star-tracker. Its function is to mark the line of sight to a single guide star. Its angular resolution, therefore, instead of depending, as in an astronomical telescope, on the Rayleigh criterion for separating the diffraction images of two nearby stars, depends on how well the telescope can locate the center of a single star image with respect to the optic axis. With a sufficiently bright star such as Rigel there is, as we will show below, no difficulty in principle in obtaining the submarc-s resolution needed for the experiment. Nevertheless the overall requirement, being two to three orders of magnitude beyond the performance of typical very good star-trackers, is formidable. The hope for such a large improvement comes from the combination of space flight and cryogenic techniques. The main factors limiting earth-based telescopes are three: (1) atmospheric turbulence, (2) distortion and creep of the structure under its own weight, (3) distortion due to temperature gradients. Operation in space eliminates the first two; operation at liquid helium temperatures eliminates the third. One cannot reap the potential improvements merely by taking an existing star-tracker and putting it in liquid helium, however. Many other points have to be considered before reaching the final design.

Given the basic decision to use a cryogenic star-tracker two further issues arise: (1) the provision of adequately stable and precise referencing of the gyroscopes to the telescope, (2) the relationship between the design of the telescope and the design of the spacecraft's pointing control system. Each issue has several subissues which affect final choices on matters such as the aperture, focal length, stability, linear range, noise performance and method of scale factor calibration for the telescope. Throughout the design our policy has been one of extreme conservatism. Everywhere we have allowed not one but at least two and in some instances three lines of defense against error. We embrace caution for two reasons. First, since there is only one telescope in the experiment, it, unlike the gyroscopes, is a potential source of common mode error. We wish to be able to prove compellingly that any errors it introduces are very much less than a marc-s. Second, recognizing that last minute compromises are often forced upon one in the development of a flight instrument, we want a large margin in hand.

We began work on the telescope in 1965. Preliminary theoretical analysis and experimental design soon revealed that the critical problem lay in dividing and reading out the image, so we set up a test stand comprising a model single axis telescope and artificial star to evaluate various image dividers and light-chopping assemblies. Experiments with the test stand in 1967 and 1968 encouraged us to go ahead in 1970 with the design of a laboratory version of the telescope. After fabrication was complete in 1972 the next question was how an instrument with potentially submarc-s precision was to be tested. Either the errors of the test device had to be less than those of the telescope or some way had to be found of separating errors from the two sources. We began design of a star/collimator unit in 1972 and completed its fabrication and assembly in December 1975. Tests carried out in 1977 and 1978, and described below, satisfied us that the telescope met most of the requirements for the experiment. Since 1979 other activities on Gravity Probe B have precluded further telescope work except for the shake test of a structural model, also described below, performed in 1982 in collaboration with NASA Marshall Center. We expect soon to resume optical tests on the laboratory telescope and to commence design of the final flight instrument.

Overview of the design

As explained earlier, the design of the telescope cannot be treated in isolation from considerations of gyroscope performance, spacecraft pointing and science data instrumentation. These considerations, which are somewhat complex, established a certain rationale for the design, to be explained in the next section, given which we defined in 1969 five performance goals for the telescope[7], as presented in the second column of Table 1. Seen

interest is in referring the gyroscope to Rigel, not in measuring the orientation of the quartz block in which the gyroscopes are mounted. This consideration led Pugh[5] early on, and later independently Kaspar and Frisch[6], to propose schemes for experiments in which the optical system would form an integral part of the gyroscopic object, allowing the quantity of interest to be determined directly using a single readout device, instead of as in our experiment through the subtraction of gyroscope signals from telescope signals. Ingenious as their suggestions were, we prefer the less direct approach. To reach the ultimate in gyro drift performance one needs a spinning body of extreme roundness and homogeneity; attempts to incorporate the optics into the gyro rotor inevitably compromise this. Also, any such scheme leads to having a single very large gyroscope operated as a drag-free proof mass, losing one of the most attractive features of the present GP-B design - the ability to make cross-checks between four different gyroscopes operating under similar but not identical conditions. For these and other more technical reasons we favor having an independent telescope.

The telescope required is, of course, a star-tracker. Its function is to mark the line of sight to a single guide star. Its angular resolution, therefore, instead of depending, as in an astronomical telescope, on the Rayleigh criterion for separating the diffraction images of two nearby stars, depends on how well the telescope can locate the center of a single star image with respect to the optic axis. With a sufficiently bright star such as Rigel there is, as we will show below, no difficulty in principle in obtaining the submarc-s resolution needed for the experiment. Nevertheless the overall requirement, being two to three orders of magnitude beyond the performance of typical very good star-trackers, is formidable. The hope for such a large improvement comes from the combination of space flight and cryogenic techniques. The main factors limiting earth-based telescopes are three: (1) atmospheric turbulence, (2) distortion and creep of the structure under its own weight, (3) distortion due to temperature gradients. Operation in space eliminates the first two; operation at liquid helium temperatures eliminates the third. One cannot reap the potential improvements merely by taking an existing star-tracker and putting it in liquid helium, however. Many other points have to be considered before reaching the final design.

Given the basic decision to use a cryogenic star-tracker two further issues arise: (1) the provision of adequately stable and precise referencing of the gyroscopes to the telescope, (2) the relationship between the design of the telescope and the design of the spacecraft's pointing control system. Each issue has several subissues which affect final choices on matters such as the aperture, focal length, stability, linear range, noise performance and method of scale factor calibration for the telescope. Throughout the design our policy has been one of extreme conservatism. Everywhere we have allowed not one but at least two and in some instances three lines of defense against error. We embrace caution for two reasons. First, since there is only one telescope in the experiment, it, unlike the gyroscopes, is a potential source of common mode error. We wish to be able to prove compellingly that any errors it introduces are very much less than a marc-s. Second, recognizing that last minute compromises are often forced upon one in the development of a flight instrument, we want a large margin in hand.

We began work on the telescope in 1965. Preliminary theoretical analysis and experimental design soon revealed that the critical problem lay in dividing and reading out the image, so we set up a test stand comprising a model single axis telescope and artificial star to evaluate various image dividers and light-chopping assemblies. Experiments with the test stand in 1967 and 1968 encouraged us to go ahead in 1970 with the design of a laboratory version of the telescope. After fabrication was complete in 1972 the next question was how an instrument with potentially submarc-s precision was to be tested. Either the errors of the test device had to be less than those of the telescope or some way had to be found of separating errors from the two sources. We began design of a star/collimator unit in 1972 and completed its fabrication and assembly in December 1975. Tests carried out in 1977 and 1978, and described below, satisfied us that the telescope met most of the requirements for the experiment. Since 1979 other activities on Gravity Probe B have precluded further telescope work except for the shake test of a structural model, also described below, performed in 1982 in collaboration with NASA Marshall Center. We expect soon to resume optical tests on the laboratory telescope and to commence design of the final flight instrument.

Overview of the design

As explained earlier, the design of the telescope cannot be treated in isolation from considerations of gyroscope performance, spacecraft pointing and science data instrumentation. These considerations, which are somewhat complex, established a certain rationale for the design, to be explained in the next section, given which we defined in 1969 five performance goals for the telescope[7], as presented in the second column of Table 1. Seen

from our present vantage point some of the goals thus defined were unnecessarily restrictive while others were not restrictive enough. Column 3 of Table 1 shows current choices, discussed further below. Not restrictive enough among the original requirements was the limitation of error to 1 marc-s, for in an experiment to measure relativity effects to 1 marc-s/yr,

Table 1: performance goals for the GP-B star-tracker

	as defined in 1969	current choices (1986)
readout alignment	two axis, alignment to gyro readout planes within a few arc-s	two axis, alignment to gyro readout planes to within 5 arc-s
null stability	absolute over a year to 1 marc-s	over 10 min roll period to 0.1 marc-s
linearity	1 marc-s over ±50 marc-s	0.1 marc-s over ±70 marc-s
resolution	50 marc-s in 10 Hz bandwidth	3 marc-s in 10 Hz bandwidth
acquisition range	±2 arc-min	±2 arc-min
automatic gain control	referred to gyroscope 1% over ±50 marc-s	referred to gyroscope 0.3% rms over ±70 marc-s

a proper error budget will have individual terms well below that level. We now set the total telescope error at 0.3 marc-s, which means an allowance for individual terms closer to 0.1 marc-s. On the other hand, with a rolling spacecraft the requirement of 1 marc-s stability for the telescope null over the one year duration of the mission is unnecessarily restrictive and has been relaxed. Nevertheless for reasons to be discussed later we retain some conservatism on null stability, as well as in all other aspects of the design.

Optical layout

Figure 1 illustrates the general optical layout of the completed telescope. It has folded Schmidt-Cassegrainian optics, with 150 in focal length and 5.6 in aperture. The

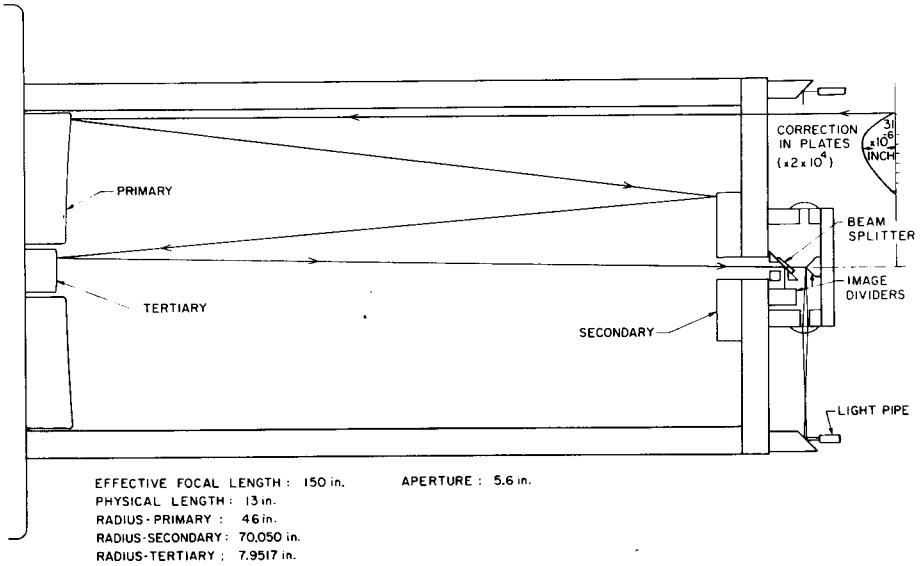

Figure1: optical layout of cryogenic telescope

physical dimension are: overall length 14 in, outside diameter 7.25 in. The parts are made entirely of fused quartz, held together by "optical contacting", that is, by direct molecular adhesion of the quartz parts. No cements or mechanical attachment devices are used, although for reasons explained below in the section on optical contacting, for the flight model we may decide to use fritting rather than contacting at the joint where the telescope tube is attached to the bottom plate. The one unconventional feature of the optical layout is that the light path is folded to put the focal plane just above the corrector plate instead of below the primary mirror as in a standard Cassegrainian telescope. This arrangement has five advantages in that it

(1) leaves the bottom surface of the telescope clear for attachment to the quartz block in which the gyroscopes are mounted.

interest is in referring the gyroscope to Rigel, not in measuring the orientation of the quartz block in which the gyroscopes are mounted. This consideration led Pugh[5] early on, and later independently Kaspar and Frisch[6], to propose schemes for experiments in which the optical system would form an integral part of the gyroscopic object, allowing the quantity of interest to be determined directly using a single readout device, instead of as in our experiment through the subtraction of gyroscope signals from telescope signals. Ingenious as their suggestions were, we prefer the less direct approach. To reach the ultimate in gyro drift performance one needs a spinning body of extreme roundness and homogeneity; attempts to incorporate the optics into the gyro rotor inevitably compromise this. Also, any such scheme leads to having a single very large gyroscope operated as a drag-free proof mass, losing one of the most attractive features of the present GP-B design - the ability to make cross-checks between four different gyroscopes operating under similar but not identical conditions. For these and other more technical reasons we favor having an independent telescope.

The telescope required is, of course, a star-tracker. Its function is to mark the line of sight to a single guide star. Its angular resolution, therefore, instead of depending, as in an astronomical telescope, on the Rayleigh criterion for separating the diffraction images of two nearby stars, depends on how well the telescope can locate the center of a single star image with respect to the optic axis. With a sufficiently bright star such as Rigel there is, as we will show below, no difficulty in principle in obtaining the submarc-s resolution needed for the experiment. Nevertheless the overall requirement, being two to three orders of magnitude beyond the performance of typical very good star-trackers, is formidable. The hope for such a large improvement comes from the combination of space flight and cryogenic techniques. The main factors limiting earth-based telescopes are three: (1) atmospheric turbulence, (2) distortion and creep of the structure under its own weight, (3) distortion due to temperature gradients. Operation in space eliminates the first two; operation at liquid helium temperatures eliminates the third. One cannot reap the potential improvements merely by taking an existing star-tracker and putting it in liquid helium, however. Many other points have to be considered before reaching the final design.

Given the basic decision to use a cryogenic star-tracker two further issues arise: (1) the provision of adequately stable and precise referencing of the gyroscopes to the telescope, (2) the relationship between the design of the telescope and the design of the spacecraft's pointing control system. Each issue has several subissues which affect final choices on matters such as the aperture, focal length, stability, linear range, noise performance and method of scale factor calibration for the telescope. Throughout the design our policy has been one of extreme conservatism. Everywhere we have allowed not one but at least two and in some instances three lines of defense against error. We embrace caution for two reasons. First, since there is only one telescope in the experiment, it, unlike the gyroscopes, is a potential source of common mode error. We wish to be able to prove compellingly that any errors it introduces are very much less than a marc-s. Second, recognizing that last minute compromises are often forced upon one in the development of a flight instrument, we want a large margin in hand.

We began work on the telescope in 1965. Preliminary theoretical analysis and experimental design soon revealed that the critical problem lay in dividing and reading out the image, so we set up a test stand comprising a model single axis telescope and artificial star to evaluate various image dividers and light-chopping assemblies. Experiments with the test stand in 1967 and 1968 encouraged us to go ahead in 1970 with the design of a laboratory version of the telescope. After fabrication was complete in 1972 the next question was how an instrument with potentially submarc-s precision was to be tested. Either the errors of the test device had to be less than those of the telescope or some way had to be found of separating errors from the two sources. We began design of a star/collimator unit in 1972 and completed its fabrication and assembly in December 1975. Tests carried out in 1977 and 1978, and described below, satisfied us that the telescope met most of the requirements for the experiment. Since 1979 other activities on Gravity Probe B have precluded further telescope work except for the shake test of a structural model, also described below, performed in 1982 in collaboration with NASA Marshall Center. We expect soon to resume optical tests on the laboratory telescope and to commence design of the final flight instrument.

Overview of the design

As explained earlier, the design of the telescope cannot be treated in isolation from considerations of gyroscope performance, spacecraft pointing and science data instrumentation. These considerations, which are somewhat complex, established a certain rationale for the design, to be explained in the next section, given which we defined in 1969 five performance goals for the telescope[7], as presented in the second column of Table 1. Seen

from our present vantage point some of the goals thus defined were unnecessarily restrictive while others were not restrictive enough. Column 3 of Table 1 shows current choices, discussed further below. Not restrictive enough among the original requirements was the limitation of error to 1 marc-s, for in an experiment to measure relativity effects to 1 marc-s/yr,

Table 1: performance goals for the GP-B star-tracker

	as defined in 1969	current choices (1986)
readout alignment	two axis, alignment to gyro readout planes within a few arc-s	two axis, alignment to gyro readout planes to within 5 arc-s
null stability	absolute over a year to 1 marc-s	over 10 min roll period to 0.1 marc-s
linearity	1 marc-s over ±50 marc-s	0.1 marc-s over ±70 marc-s
resolution	50 marc-s in 10 Hz bandwidth	3 marc-s in 10 Hz bandwidth
acquisition range	±2 arc-min	±2 arc-min
automatic gain control	referred to gyroscope 1% over ±50 marc-s	referred to gyroscope 0.3% rms over ±70 marc-s

a proper error budget will have individual terms well below that level. We now set the total telescope error at 0.3 marc-s, which means an allowance for individual terms closer to 0.1 marc-s. On the other hand, with a rolling spacecraft the requirement of 1 marc-s stability for the telescope null over the one year duration of the mission is unnecessarily restrictive and has been relaxed. Nevertheless for reasons to be discussed later we retain some conservatism on null stability, as well as in all other aspects of the design.

Optical layout

Figure 1 illustrates the general optical layout of the completed telescope. It has folded Schmidt-Cassegrainian optics, with 150 in focal length and 5.6 in aperture. The

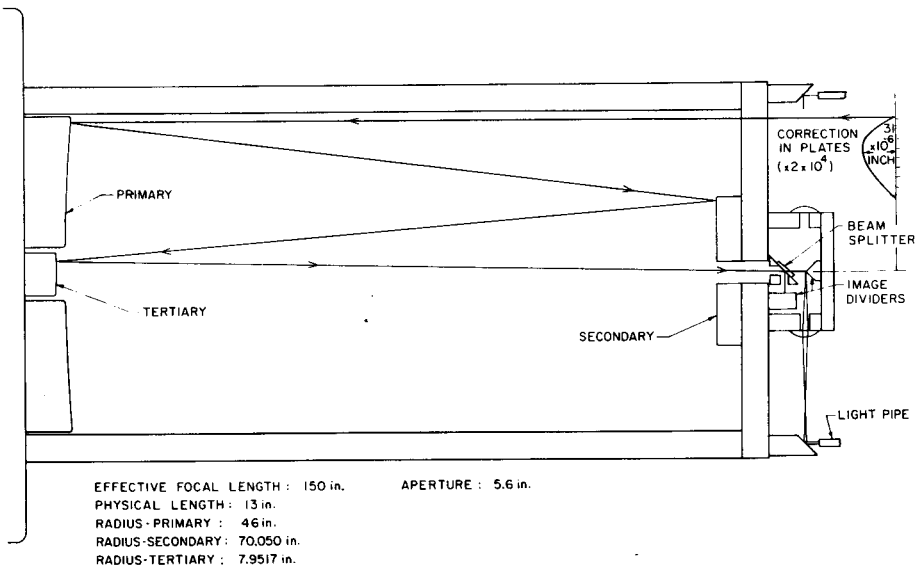

Figure1: optical layout of cryogenic telescope

physical dimension are: overall length 14 in, outside diameter 7.25 in. The parts are made entirely of fused quartz, held together by "optical contacting", that is, by direct molecular adhesion of the quartz parts. No cements or mechanical attachment devices are used, although for reasons explained below in the section on optical contacting, for the flight model we may decide to use fritting rather than contacting at the joint where the telescope tube is attached to the bottom plate. The one unconventional feature of the optical layout is that the light path is folded to put the focal plane just above the corrector plate instead of below the primary mirror as in a standard Cassegrainian telescope. This arrangement has five advantages in that it

(1) leaves the bottom surface of the telescope clear for attachment to the quartz block in which the gyroscopes are mounted.

(2) provides an easy path to the outside world for the emergent light beams.

(3) allows for incorporating a light baffle (not shown) of very efficient design at the hole in the secondary mirror, thus eliminating any stray light that has gotten past the external sunshield illustrated in Figure 2 of the accompanying paper by L.S. Young.[3]

(4) simplifies the design of the corrector plate.

(5) reduces the physical length of the telescope needed for a given focal length.

The last advantage is one of practice rather than of principle. Theoretically there is no limit to the focal length of a Cassegrainian telescope. It is simply a matter of choosing the right magnification ratio. In practice there is a limit, however, because difficulties in making the secondary mirror mean that any increase in focal length beyond a certain point cause deterioration of image quality. Having an extra stage of magnification eases the problem.

Angular readout is obtained as follows. A beam-splitter, located about an inch in front of the focal plane, forms two star images, one for each readout axis. Each image then falls on the sharp edge of a roof prism where it is again subdivided into two half images. Measurements of the relative intensities of each pair of half images determine the angles from the two readout planes to the line of sight to the star. Practical considerations underlie the choice of two roof prisms to divide the image rather than a four-sided pyramid or other quadrant detector. The manufacturing tolerances are too severe for any other device we have been able to think of. This issue is discussed further in the section on rationale,and Equation(12) of the theoretical analysis sets the limit on the sharpness of the dividing edge.

The beam splitter and roof prisms are optically contacted into a "light-box" mounted in the middle of the corrector plate, just over the central obscuration caused by the presence of the secondary mirror. Since the beam splitter introduces astigmatism in its transmitted beam, the prisms are mounted in such a way as to make the elongation in the transmitted image parallel to the roof line of the prism that divides it. Lenses attached to the light-box refocus the beams, which pass to small 45° mirrors at the side of the telescope and hence via light-pipes to detectors at room temperature or, in the flight experiment, ambient satellite temperature.

For reasons discussed below in the sections on rationale and theoretical analysis we decided to operate the telescope in focus, that is, with the star-images focused on the edges of the roof prisms. With diffraction limited optics the image diameter, defined to the region of maximum slope in the diffraction pattern, is given by the Airy expression $1.22\ \lambda/D$, which yields for green light a diameter of 0.94 arc-s or in linear measure 0.68 mil. The diameter to the first diffraction minimum is just twice this value.

Chopper-detector assembly

The two axes have independent detection systems, each consisting of a photomultiplier and chopper so arranged that signals from the paired light-pipes are presented successively on the same area of the photocathode. Thus zero drifts due to aging of the cathode material are avoided. The signals are amplified and synchronously demodulated in a circuit which includes an automatic gain control and other special features described below.

Figure 2 illustrates the chopper-detector developed for the laboratory version of the telescope. It consists of a 3 in diameter rotating disk with four slots, two for the readout signals and two with small lamps and diode detectors to provide timing signals for synchronous demodulation. To eliminate stray light, the photodetector and chopper form a single unit with intersecting light baffles in the rotating disk and the case. The chopping frequency is 50 Hz. The first design had pairs of f/3 lenses to focus the emergent beams from the light pipes and transmit them to the detector. Heavy light losses resulted. After many trials we eliminated the lenses and made the distance from light-pipe to photocell as short as possible, tilting the ends of the pipes toward each other as illustrated in Figure 2 in order to have the output beams superimposed. This overlapping of the beams is important. Over the course of a year in space the sensitivity of a typical photomultiplier may decay by as much as 60%. Assume a variation of 20% in aging across the cathode, i.e. that the decay ranges from 54% on one side to 66% on the other. With an image diameter of 1.8 arc-s the output beams have to overlap on the cathode by 90% to ensure that there is no null shift greater than 1 marc-s.

Some details of the present chopper design were determined by the exigencies of the laboratory set up. One problem was the magnetic shielding and cooling of the drive motor. When the chopper is run in air the viscous drag in the closely intersecting light baffles

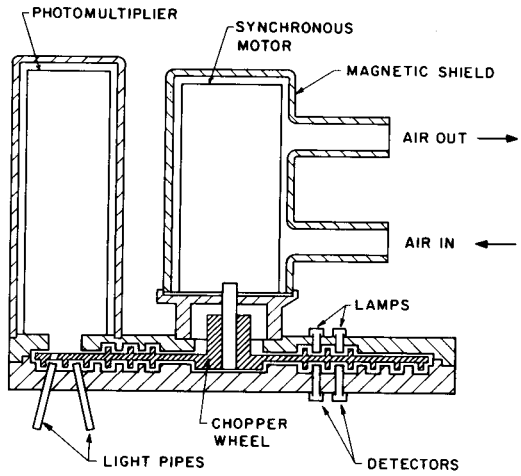

Figure 2: chopper-detector assembly

is surprisingly large. Hence the drive motor has to be more powerful than one might expect (10W), and since it is surrounded by a magnetic shield (to minimize its magnetic effects on the gyroscope), it has to be cooled by a forced draft obtained from an external source of air. Several features could and should be changed in a flight version, though even the flight version must be designed to work in ground tests. One obvious improvement would be to take the timing signals from capacitative measurements on slots milled in the chopping wheel rather than from lamps and diode detectors. The wheel would than be smaller, with fewer light baffles and less drag. More generally one might consider replacing the wheel by a vibrating reed detector. Included in the design considerations must be a study of the effects of vibrations on the relativity gyroscopes, and the effects of the gyroscopic action, if any, of the choppers on the spacecraft pointing controller.

The photomultiplier used in the first experimental detector was a 1P21 with a 20 KΩ load resistor. The present detection system uses 4441A photomultipliers, specially selected for high sensitivity and initially matched to 10% in the two channels. The 4441A has a lower inherent gain than the 1P21 but has two advantages. Its quantum efficiency is higher (15% as compared with 12%), and its configuration, being end on rather than sideways, allows the photocathode to be closer to the ends of the light-pipes, reducing the optical losses. The performance of various sensors are compared below in the theoretical analysis section.

Readout electronics

The preliminary experiments on the single axis simulator were performed with a preamplifier/demodulator circuit designed in 1968 by R.A. Van Patten. In 1977 R.R. Clappier designed an updated version with separate channels for the x and y telescope readout axes using CMOS analog switches for demodulation. The newer circuit was designed to consume very little power, making it suitable for space application. It was used in the telescope tests described below.

In the preliminary experiments we observed a serious zero error, arising from asymmetry in the shapes of the transition regions at the 0° and 180° phase points derived from the light-chopper. The magnitude of the error varied with both the amplifier gain and the position of the star image. Two steps were taken to remove it. The ends of the slots in the chopping wheel were carefully shaped to minimize the spikes in the photomultiplier output arising in periods of overlap or underlap. The timing for the CMOS analog switches was implemented in such a way as to blank out the signal in a small time range around each transition. A chopper giving smooth transitions is needed even with a blanking circuit because the amplifier operates continuously and is subject to overload disturbances, which might persist long enough to cause error if there were appreciable spikes in the input. Time symmetry was guaranteed by using common logic circuits to blank out both transition regions. The circuit was designed to ensure voltage symmetry of the signal by blocking the d.c. bias present in the photomultiplier output.

With these and other improvements the circuit operated successfully and telescope signals were resolved to the marc-s level.

Rationale of the design

Some points in the foregoing design are self-evident; others, notably the choice of detection scheme, have aroused question. Without claiming finality we offer here a broad statement of our reasons for taking the approach we have, concentrating on the two issues identified in our introduction - precise referencing of the gyroscopes to the telescope, and the relationship between telescope design and spacecraft pointing. We begin with mechanical stability, than discuss pointing control, and finally come back to questions of optical and electronic stability. Details on noise performance, linearity and other such matters are deferred to the theoretical section.

Mechanical stability

Let us replace the 1 marc-s criterion of 1969 by the more stringent and correct requirement that errors from angular displacements between the gyro and telescope readouts should be kept below 0.1 marc-s or 4.8×10^{-10} rad. With a telescope of 150 in focal length and 5.6 in aperture, a tilt of 4.8×10^{-10} rad corresponds to the following distortions of the telescope/quartz block structure: motion of star-image at focal plane $\sim$ 18 Å, tipping of primary mirror across its diameter $\sim$ 0.7 Å, tipping of gyro housing across the diameter of a readout ring $\sim$ 0.2 Å. It is through considering the minuteness of these displacements that we arrive at the idea of having a telescope fabricated entirely of fused quartz, held together by fritting or optical contacting rather than by means of cements whose dimensions might change with age, and attached to a massive quartz block containing the gyroscopes, as illustrated in Figure 6 of the paper by Bardas et.al.

With this as the basic plan we examine the effects of distortions from external accelerations, creep and thermal gradients. On earth, with the telescope cantilevered horizontally, sag under the 1 g acceleration can be shown to displace the star image by 130 marc-s. In space, where the drag-free control system keeps lateral accelerations on the spacecraft below 10^{-10}g, the acceleration-induced flexure is utterly negligible. Similarly for acceleration-induced creep. Assume, as is near enough for this purpose, that creep under external load can be represented by the classical Maxwell model. Its value can be estimated by applying Trouton's similarity principle, according to which the creep θ_C over time t of a structure whose flexure under load is θ_E, is given by $\theta_C = \theta_E t/\tau$, where τ is a relaxation time equal to η/E, the ratio of viscosity to elasticity for the material. For fused quartz at low temperatures τ certainly exceeds 100 years,[8] so over one year the acceleration-induced creep will be two orders of magnitude smaller than the already negligible elastic flexure.

Potentially more significant are creep from stresses in the quartz block mounting flange caused by the retaining forces from the probe support structure (Figure 6 of Bardas et.al.), and the relaxation by the delayed elastic effect of any asymmetrical stresses built up in the telescope/quartz block assembly during manufacture. The former is minimized by making everything axially symmetric; its likely magnitude can be estimated by using an autocollimator to observe the elastic distortion, if any, from tightening the flange, and again applying Trouton's principle. Delayed elastic effects are significantly smaller at low temperatures than at room temperature. More important, they can be made benign by annealing the telescope/quartz block structure in a vertical orientation after manufacture, in which case their only effect will be an utterly negligible slow change in the telescope's focal length over the course of the year. The components that matter are the quartz block and the telescope tube, each of which can be annealed separately before final assembly, 24 hours at 800°C being amply sufficient. Details are given elsewhere.[9] If the telescope/quartz block structure had to be stored for long periods before flight, there would be some wisdom in storing it vertically.

A thermal gradient transverse to the axis of the telescope warps it, displacing the star image by an amount given by Equation(13) below. Numerical calculations, also summarized below (Table 3), show that whereas the errors may be large in a room temperature telescope, in a cryogenic telescope they are negligible.

Thus we may have good confidence that the telescope/quartz block structure will remain mechanically stable to better than a marc-s over the course of a year. This is our first line of defense. But to make assurance double sure we roll the spacecraft with 10 min period about the line of sight to the guide star, so that even if some long-term change in figure does occur, its effect will vanish out of the relativity data. The many other functions of spacecraft roll are indicated in the paper by Bardas et.al. Seeing how powerful the roll principle is one might tend to wave away elaborate considerations of the telescope's mechanical stability as superfluous. We think otherwise. Principles like roll

averaging are good servants but bad masters. If we are to maintain good margins on the errors in Gravity Probe B, we need to be very selective about the areas in which we place the burden on roll. There is a big difference between averaging out a last factor of two and averaging factors of 10^4 or 10^5, for in the latter secondary rectifying effects may become appreciable. Also the fewer terms one is relying on roll-averaging for, the easier it will be to carry out a diagnostic process (in-flight calibration) to verify its effectiveness.

To take a specific example where roll-averaging would not automatically remove an error, consider the issue of thermal distortion in a room temperature telescope. Sunlight falling on the side of the spacecraft makes the telescope warp away from the sun. Rolling the spacecraft tends to wash out this effect, but not entirely because the heat flux is coming from a fixed direction in inertial space. The magnitude of the inertially fixed "hot-dogging" depends on the ratio of the roll-period to the thermal time constants of the system; it is extremely difficult to reduce the offsets to 0.1 marc-s. With a cryogenic telescope there is no such worry.

Relationship between spacecraft pointing and telescope design

Our first consideration in analyzing the pointing problem must be to ask what it is we are trying to point at. In testing relativity our concern is the angle between the gyro spin axis and the line to what may be called the "true" position of the guide star. But that is not what we observe. The observed line of sight is to an "apparent" position of the star which varies from the true position by upwards of 23 arc-s as the result of

.annual aberration in the plane of the ecliptic amounting to ±20.492 arc-s

.parallax also in the plane of the ecliptic, amounting to approximately ±7 marc-s and 90° out of phase with the annual aberration

.orbital aberration in the plane of the satellite orbit, amounting to approximately ±5 marc-s

.relativistic deflection of starlight by the sun, having (with Rigel as guide star) a maximum value of 14.4 marc-s away from the sun on June 10th of each year

These signals have to be separated from the relativistic precessions of the gyroscopes. Fortunately the separation is easily made from the different time signatures of the signals: the star displacements all have annual or orbital periodicity, the relativity drifts of the gyroscopes vary linearly with time.

Evidently the combined signals can be taken up in any one of three ways: (i) all in the gyro readout, (ii) all in the telescope readout, (iii) in some combination of gyro and telescope readouts. With method (i) the pointing control would be referred to the telescope; with method (ii) it would be referred to the relativity gyroscopes; with method (iii), which is the only one that could allow the spacecraft to point to the "true" direction of the star, some additional input would be needed and the gyro and telescope readouts would both have to have wide linear range. And this brings us to the crux of our problem. Whatever decision we take at least one of the two readouts must have linearity approaching 0.1 marc-s over a dynamical range of ±50 arc-s* in order to be able to process the combined relativity and aberration signals, plus an allowance (10 arcs, say) for null offset between it and the other readout. The precision required is around 18 bits - about the limit on the present state of the electronic art. For the gyro readout, which is based on measuring an electric current proportional to the tilt angle, the task is not unduly difficult; for the telescope readout it is almost impossible. We have indeed examined some suggested designs for precise wide angle telescope readouts (e.g. the use of encoded tipping plates in the converging beam and a method[10] based on displacing the image divided piezoelectrically and measuring its displacement with an interferometer) but they are fraught with difficulty - especially in a cryogenic environment. Our preference is, therefore, to point the telescope at the apparent position of the guide star and take up the full range of signals in the gyro readout.

It would be illusory, however, to think that one could point the spacecraft to a marc-s. Our goal must be a total system design for telescope, gyroscope and pointing control that will satisfy the experiment requirements. And that means two things: adequate linearity of the telescope readout, and sufficiently close matching of the scale factors for the gyroscope and telescope readouts. Suppose the pointing control system can keep the space-

* There is a sense in which this statement is not true. One might imagine feeding back electrical signals into the readout that would just cancel the expected aberration and relativity signals, thus reducing the required linear range. However the task of providing the cancelling signals is as great as, or greater than, the task of providing (for the gyroscope, at least) a readout of adequate range.

craft on the apparent line of sight to Rigel to within an angular range θ_p. Then the telescope readout should be linear to 0.1 marc-s over a range $R < \theta_p$. Again, suppose that the gyroscope output is such that the ratio of the angle it records to the true angle is C_G, while the corresponding ratio for the telescope is C_T, with C_G and C_T each being nominally unity. Then if the spacecraft were mispointed by θ_P ($< \theta_p$), there would be a measurement error $\delta\theta$ equal to $(C_G - C_T)\theta_p$. Take θ_p as 30 marc-s. To keep $\delta\theta$ below 0.1 marc-s the ratio $(C_G - C_T)/C_G$ would have to be kept below 0.3% rms.

A procedure for scale factor matching has been devised by R.A. Van Patten. It consists in injecting into the spacecraft pointing system a "dither" signal that makes it oscillate back and forth across the line of sight to Rigel with (say) a 1 min period and an amplitude of 20 marc-s. This signal will appear in both gyro and telescope outputs. Suppose the two outputs are subtracted, either in an on-board data instrumentation system or in the ground-based Kalman filter described in the accompanying paper by Van Patten, DiEsposti and Breakwell.[11] If the scale factors are matched the dither signal will vanish from the subtracted output, but if they are not matched a sinusoidal signal will appear, whose amplitude and phase supply a measure of $(C_G - C_T)$. This signal may be applied in an on-board automatic gain control circuit to adjust the telescope scale factor to match that of the telescope, or alternatively, an equivalent process may be implemented in the ground-based Kalman filter.

The issues of linearity, noise performance, pointing control design and scale factor matching are evidently all bound up together. In any control system the ultimate limit on control performance is the sensor noise. Hence to be acceptable the noise equivalent angle δ_ν of the telescope at the bandwidth of the controller must be significantly less than the telescope's linear range R. But, as will be shown below, δ_ν and R are related to each other. Suppose one tries to increase R by defocusing the star image (Equation (4)). According to Equation (8) δ_ν also increases - more rapidly than R. Also, the greater R is the more stringent is the requirement on the matching of C_G and C_T; and matching too is limited by a noise, the noise in the gyro readout. Attempts to enhance the linear range by other means such as an image compensating device prove equally fallacious, though having an image compensator or an inner pointing servo steering the telescope/quartz block structure may ease the pointing problem. We conclude that the best systems design will have a focused star image, with diameter set by the diffraction limit of the telescope. The control issue is then to design a pointing servo for which $\theta_p < R$.

Note that in specifying the requirements on linearity and scale factor matching we have, as hinted earlier, allowed ourselves two additional lines of defense against error. First, the 0.1 marc-s requirement is specified in each case for the maximum pointing error θ_p, whereas in reality the pointing errors θ_p will have some roughly Gaussian distribution about the null (though conceivably there might be short-term biases in the pointing control error). Second, there is the averaging from roll. A full discussion would require a statistical model of pointing errors and the effects of roll applied to an analysis incorporating telescope aberration terms. This we have not yet attempted.

Optical and electronic stability, and method of dividing the image

The use of a focused image has another advantage: it minimizes null shifts due to aging of the telescope optics. With an out-of-focus instrument one is looking essentially at the geometrical image of the aperture, and any differential aging from effects such as ultraviolet darkening of the quartz windows in the dewar neck-tube or changes in reflectance of the mirrors, will cause a first order null shift. To maintain absolute stability to 0.1 marc-s with an image defocused to 10 arc-s diameter, the differential aging could not be allowed to exceed a part in 10^5 of the total light transmittance, that is, with an overall change of 1% the difference across the image would have to be below 0.1%. (The errors from such long-term null shifts are, of course, very effectively averaged by spacecraft roll.) With a focused image the shift is reduced for two reasons: the image is smaller and the relative displacement is made second order because there is no longer a one-to-one correspondence between elements in the aperture and elements in the diffraction image. Thus even without spacecraft roll the resultant shifts are negligible. On the other hand null shifts can occur through differential aging of the light-pipes or of the coatings on the roof prisms. Such effects are inherently likely to be smaller than changes over the telescope aperture, and are minimized by using a focused image; nevertheless they could exceed 0.1 marc-s. If so we have to rely on roll-averaging to remove them.

This brings us to our next point, the decision to divide the star image by means of a roof-prism. An alternative method often used is to chop the image at the focal plane, either by a vibrating reed or a rotating disk. Such schemes eliminate the null offset due to aging of light-pipes, and we are sometimes asked why one of them was not adopted. A first answer is that reliable cryogenic choppers are hard to come by. Even more fundamental, however, is the difficulty of meeting the 18 Å requirement on the transverse stability at the focal plane. Take, as a specific example, a knife edge mounted in a rotating cylinder of metallized quartz supported in an electrostatic bearing similar in

design to the gyro suspension system. From experience with the gyroscope we know that the long-term centering stability of a well-designed suspension system is about 5 μin or 1300 Å - a factor of 70 worse than our requirement. This alone is a significantly greater burden than anything to be expected from aging of the light-pipes. Moreover the temperature-dependences of the electronics open the way to errors that rectify as the spacecraft rolls in the sunlight. With the existing gyro suspension a temperature change of 18°C produces a displacement of 5 μin. To prevent a telescope null shift of 0.1 marc-s in a fixed direction in inertial space the temperature of the electronics would have to be controlled to about 0.25°C over a roll period. Thus a rotating chopper has no advantage and several disadvantages. Similar considerations, given elsewhere,[12] make a vibrating reed equally unattractive.

Going to the opposite extreme, some people have suggested that roll-averaging is so powerful that using a chopper-detector to measure the output of the light-pipes is unnecessarily conservative. Why not have two separate photodetectors and let roll take out the long-term null drifts? Besides general caution, we have a second reason for wanting to stay with the chopper: it improves the performance of the telescope by eliminating 1/f noise from the output. Furthermore, just as with the rotating knife-edge one must worry about rectifying offsets due to temperature changes in the electronics, so with separate photodetectors one would have to worry about the offsets from roll synchronous changes in detector gain, due for example to a temperature dependence in the circuit producing the drive voltage. With a chopper such changes would affect the overall scale factor of the telescope, and allowance would have to be made for that, but they would not cause null offsets.

Effect of the companion of Rigel

The theory of the telescope developed below assumes an ideal isolated guide star. Rigel has a companion about 9.4 arc-s away, whose brightness is 1/400 of the main star. The effect is to throw extra light into one side of the readout channel, causing a null shift of ±1.3 marc-s (for a focused image), the sign of which changes as the spacecraft rolls through 180°. The error vanishes in data analysis after averaging over an even number of half-rolls. The shifts are, of course, 90° out of phase in the two readout axes.

Thus the companion of Rigel has no significance in the experiment. If one tried to use a guide star which had a companion more nearly equal to it in brightness, however, the image could become displaced into its nonlinear region with unfortunate results. In the extreme, with two sources of equal brightness separated in angle by a distance greater than the image diameter, the star-tracker would cease to work.

Theoretical analysis

We now calculate the expected linearity and noise performance of the telescope for both focused and defocused images, and obtain an expression for the minimum acceptable brightness of the guide star. We also investigate design parameters, such as the allowable temperature gradients across the telescope and the requirement on sharpness of the image dividers. For simplicity we begin with an image sufficiently defocused to be treated as a uniformly illuminated disk (with and without central obscuration) and then go to the diffraction limited image. Results for the latter depend not only on the optics but also on the spectral distribution of the starlight and the quantum response of the photodetector. Some of the investigations are due to colleagues mentioned in the text.

The existing telescope has, as already stated, an aperture of 5.6 in and a focal length of 150 in. We arrived at these figures rather subjectively, starting from what we thought was about the largest acceptable physical size for the telescope (length 14 in, outer diameter 7.25 in) and then seeing what were the greatest aperture and longest focal length that could be provided with assured manufacturing technique. In retrospect the choices seem unexpectedly good; better than could reasonably have been expected given our knowledge at the time.

Linearity

Let the power flux from the star be S W/cm^2. Then the total quantity of light entering a telescope of clear aperture D is $\pi SD^2/4$. Assume that the secondary mirror obscures a proportion $(1-\alpha)$ of the image, that the efficiency of light transmission through the optics is β $(0<\beta<1)$, and that the ratio of on-time to off-time of the light-chopper is $\gamma(\sim 0.5)$, then the mean power level at each detector is

$$E = \frac{\pi}{8}\,\alpha\beta\gamma SD^2 \qquad (1)$$

the additional factor of 1/2 being the result of having two star images.

Consider an idealized telescope without central obscuration, sufficiently out of focus for the image to be treated as a uniformly illuminated disk of diameter d. Let the disk fall on a roof prism, by which it is divided into two areas A and B. The readout measures the difference in power levels between A and B. From the geometry of a circle the power difference ε due to a displacement δ of the image is[13]

$$\varepsilon = \beta\gamma SD^2 \left(\frac{\delta}{d}\right)\left\{1 - \frac{2}{3}\frac{\delta^2}{d^2} - \frac{2}{5}\frac{\delta^4}{d^4} + \ldots\ldots\right\} \quad \text{defocused image} \tag{2}$$

where δ and d are expressed in similar units of linear or angular measure. Defining the sensitivity σ as ε/δ, expressing δ and d in arc-s, and neglecting all terms in Equation (2) except the first, we have

$$\sigma = \beta\gamma SD^2/d \quad \text{W/arc-s} \tag{3}$$

Equations (2) and (3) show that for a telescope with clear aperture defocusing reduces the sensitivity in direct proportion to the image diameter d, but improves the linearity over a given range in proportion to $1/d^2$.

If the telescope has a central obscuration from which is formed a dark spot at the center of the image of diameter c ($\sim$0.4d for our telescope) the terms δ^2/d^2 and δ^4/d^4 inside the bracket of Equation (2) should be replaced by $\delta^2(1/c^2 - 1/d^2)$ and $\delta^4(1/c^4 - 1/d^4)$, and the obscuration rather than the aperture becomes the main source of nonlinearity. However the new expressions suggest a method of correcting the nonlinearity in a defocused telescope, by replacing the circular central obscuration by a barrel-shaped one have an edge-curvature equal to D, and axes parallel to the image dividers. Then, neglecting diffraction, all higher terms in the bracket of Equation (2) vanish, and the readout will be linear over a range corresponding to the width of the barrel. Preliminary experiments in 1969 confirmed that a shaped obscuration can improve the linearity of a defocused image. Since we intend to use a focused image the chief value of this observation is as a pointer.

For an out-of-focus clear aperture telescope, the range R of operation for which deviations from linearity remain below a limit Δ is, from the second term in the bracket of Equation (2)

$$R = \pm 1.15\ \Delta^{1/3}\ d^{2/3} \quad \text{defocused image} \tag{4}$$

where R, Δ and d are expressed in similar units of linear or angular measure. Applying (4) to a circular disk equal in diameter to the diffraction image of green light for a 5.6 in aperture telescope (d = 0.94 marc-s) one finds for a Δ of 0.1 marc-s an allowable range of $\pm$51 marc-s. The corresponding range for a type A_o star at a temperature of 11000 K is $\pm$35 marc-s.

A proper treatment of readout linearity with diffraction limited optics will take into account the variation in intensity across the image. For monochromatic light the result can be expressed analytically by using a Gaussian spot as an approximation to the star image, which yields, as R.B. Emmons[14] has shown, an expression similar to (4) but with a coefficient of 0.91 instead of 1.15 - i.e. a linear range about 25% less than that obtained with the circular disk approximation. With a focused image, however, the effective diameter is no longer a free parameter but is given by the Airy formula $1.22\lambda/D$, where λ is the wavelength of the light, so instead of (4) we get

$$R = 1.04\ \Delta^{1/3}\ \lambda^{1/3}/D^{2/3} \quad \text{focused image, monochromatic light} \tag{5}$$

and the allowable range decreases with increasing aperture. For white light it is necessary to integrate over the color distribution of the star and the responsivity of the photodetector. A suitable procedure has been developed by W.L. Pondrom Jr., who obtains a response function $Y(\delta)$ for the telescope (the normalized counterpart of Equation (2)) in terms of the integral

$$Y(\delta) = \frac{2}{\pi}\int_0^{\hbar_m} M(\hbar)\ \frac{\sin \hbar\delta}{\hbar}\ d\hbar \tag{6}$$

where $M(\hbar)$ is the modulation transfer function (the Fourier transform of the intensity distribution, obtained by convoluting the telescope aperture with itself), expressed in terms of spatial frequency $\hbar$, with $\hbar_m$ being the maximum value of $\hbar$ in line pairs per rad, set by the diameter of the aperture and the shortest wavelength detectable by the photocell. For an S-11 detector $\hbar_m$ is 3×10^6; for an S-20 detector it is 2×10^6. Figure 3 gives the range-error relation Δ versus R for our telescope with a central obscuration 0.4583 times the aperture and an S-11 detector looking at a type A_o star at 11000 K. The linear range allowable with a Δ of 0.1 marc-s is about 33 marc-s, remarkably close to the value obtained from the primitive calculation based on Equation (2). The error at 50 marc-s

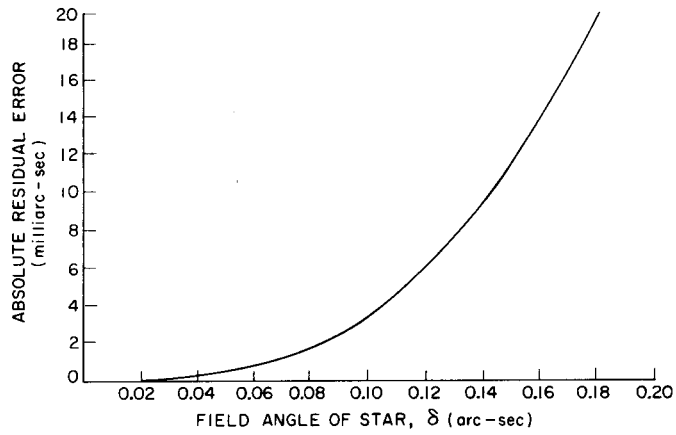

Figure 3: calculated range-error relationship for telescope

range is just under 0.5 marc-s.

Two methods exist for increasing the linear range without incurring the loss of sensitivity brought about by defocusing. One, taking a clue from the barrel-shaped obscuration, seeks to apodize the aperture in such a way as to redistribute the light into something closer to a uniformly illuminated square image. This method results in some loss of light, and hence of sensitivity, but not as much as from the corresponding degree of defocusing. The second method, due to S.B. Grossman and R.B. Emmons[15] and already applied successfully by Lockheed to another instrument, corrects the third order term in the response curve electronically. Lockheed experience suggests that with proper calibration the second method could increase the effective linear range by a factor of two: the errors should remain below 0.1 marc-s over a range of about ±70 marc-s.

Noise performance: the photon limit

Energy fluctuations in the two halves of the image, caused by random arrivals of photons, set an ultimate limit on the performance of the star-tracker. To reach the limit, other sources of noise must be eliminated by suitable choice of photodetectors and amplifying circuitry. Since this is a random noise problem, a measurement of a constant angle will evolve with time t as $t^{-\frac{1}{2}}$ provided photons noise is indeed the limit. If however, the angle is fluctuating or if 1/f noise is entering the system from elsewhere, other limits will occur. Evidently a crucial result will be the noise to be expected at the bandwidth of the pointing controller.

As with the analysis of linearity, an exact treatment would require an integration over the color distribution of the star and the response of the photodetector, but with quantum efficiency rather than gain as the relevant response function. We restrict our investigation to the simpler cases of the uniformly illuminated disk and the diffraction image formed by focused optics in monochromatic light.

Consider a disk uniformly illuminated by light of average wavelength $\bar{\lambda}$ corresponding to the color temperature of the star. Since the energy of a photon is hc/λ, the average number of photons arriving at each detector in time t is $n=E\lambda t/hc$, where E is the energy from Equation (1). The quantum noise depends not on the number of photons but on the number of photoelectrons released at the cathode of the detector, that is $(n\bar{\eta})$, where $\bar{\eta}$ is the detector's mean quantum efficiency, so the average level of the random fluctuations $\bar{\varepsilon}_\nu$ of energy between the two halves of the image is $E(n\bar{\eta})^{-\frac{1}{2}}$. Substituting for n and putting ν, the bandwidth of the receiver, for 1/t, we get $\bar{\varepsilon}_\nu=(Ehc\nu/\bar{\lambda}\bar{\eta})^{-\frac{1}{2}}$, or with numerical values for h and c

$$\bar{\varepsilon}_\nu = 4.46 \times 10^{-12}(E\nu/\bar{\lambda}\bar{\eta})^{-\frac{1}{2}} \quad W/cm^2 \qquad (7)$$

These fluctuations act effectively at the optical center of each half image, that is at a distance $d/2\pi$ from the dividing line. Define a noise equivalent angle $\bar{\delta}_\nu$ given by $\bar{\varepsilon}_\nu/2\pi\sigma$ where σ' is the sensitivity from Equation (2) multiplied by α to allow for the loss of light at the central obscuration. Combining the expressions from (1), (2) and (7) and substitu-

ting $S = 3.1 \times 10^{-14}\ 2.51^{-M}$ W/cm² as the relationship between the energy flux S of a star and its magnitude M we get

$$\bar{\delta}_\nu = 3.6 \times 10^{-6}\ (2.51^{M}\nu/\bar{H}\bar{\lambda})^{-\frac{1}{2}}\ \frac{d}{D} \qquad \text{defocused image} \qquad (8)$$

where $H = \alpha\beta\gamma\bar{\eta}$ is the total optical efficiency of the star-tracker and $\bar{\delta}_\nu$ and d are in the same units of linear or angular measure.

Equation (8) shows that with a defocused telescope the noise equivalent angle increases linearly with the image diameter d. Equation (4), on the other hand, shows that the allowable operating range R increases as $d^{2/3}$. Hence, as stated earlier, if photon noise is indeed the limiting factor on spacecraft pointing, any attempt to improve the pointing margin by defocusing the star image will be self-defeating. A focused image is best.

For the focused monochromatic image an equation corresponding to (8) is obtained by once again approximating the central portion of the diffraction pattern by a Gaussian function. The sensitivity is given by a formula corresponding to Equation (2) multiplied by $\pi^{\frac{1}{2}}/2$, and the effective image diameter by the $1.22\lambda/D$ of the Airy disk. Then $\bar{\delta}_\nu$ in arc-s is given by

$$\bar{\delta}_\nu = 1.0\ (2.51^{M}\ \bar{\lambda}\nu/\bar{H})^{-\frac{1}{2}}\ \frac{1}{D^2} \quad \text{arc-s} \qquad \text{focused image, monochromatic light} \qquad (9).$$

With focused diffraction limited optics, therefore, $\bar{\delta}_\nu$ varies as $1/D^2$, whereas with a defocused telescope and fixed image diameter, it varies only as 1/D. The difference is that the diameter of the Airy disk in the focused case decreases with increasing aperture. In both cases the resolution is improved by increasing the optical efficiency $\bar{H}$ and the integration time $\tau(=1/\nu)$. It is also improved by having small M, and in the focused case by having small $\bar{\lambda}$ as well - choosing, that is, a bright blue star.

For Rigel M is 0.7 and $\bar{\lambda}$ is about 4000 Å. The resulting photon flux is 1.6×10^6 ph/cm²-s, so with an aperture of 5.6 in (14 cm) the number of photons entering the telescope per second is 2.5×10^8. Assume a light transmission factor ($\alpha\beta$) of 0.1, a chopping factor γ of 0.5, and an effective quantum efficiency $\bar{\eta}$, allowing for aging over the mission, of 5% (in contrast to the 15% efficiency quoted above for a fresh, specially selected, S-20 detector). Then $\bar{H}$ is 2.5×10^{-3}, and the noise equivalent angle $\bar{\delta}_\nu$ in 1 s observation time is about 1 marc-s.

To avoid nonlinearities the telescope must stay pointed within the range R indicated by Equation (5) or more exactly by Figure (3). Suppose one has an ideal pointing control system with performance limited solely by the photon noise in the telescope. The telescope must satisfy the criterion $R > \bar{\delta}_{\nu_o}$, where $\bar{\delta}_{\nu_o}$ is the noise of the bandwidth ν_o of the controller, from which one sets a fundamental limit on the acceptable magnitude M_o of the guide star

$$\frac{2.51^{M_o}}{\bar{\lambda}^{1/3}} < 1.3 \times 10^{-7}\ \frac{\bar{H}}{\nu_o}\ \Delta^{2/3}\ D^{8/3} \qquad (10)$$

where Δ is in arc-s. From (10) we find that no star fainter than seventh magnitude is acceptable.

In reality a more stringent limit applies. Disturbing torques on the satellite cause pointing errors at least an order of magnitude larger than $\bar{\delta}_{\nu_o}$, i.e. larger than 10 marc-s. This in turn means that the scale factors of the gyro and telescope readouts have to be matched, as explained earlier, and since the matching is done by injecting a dither signal into the pointing controller, it requires a further increase in the linear range of the telescope. The dither amplitude is set by the matching requirement and the noise in the gyro readout; 20 marc-s is a likely figure. Combining the various needs and limitations we find that R should exceed $30\bar{\delta}_{\nu_o}$, from which we conclude that no star fainter than magnitude 4 is acceptable. Rigel, with a magnitude of 0.7, offers a good margin.

The existence of this margin leads us to qualify slightly the general statement that defocusing is not a suitable method for increasing the readout range. Defocusing may in one view be thought of as equivalent to working with a fainter star. A little (up to a 50% increase in image diameter, say) would do no harm, and might help by tending to smooth out telescope aberrations from the star image. Too much would still be bad because, as previously discussed, it would increase the danger of null shifts, and (worse) would tighten the already tight requirement on scale factor matching.

Noise performance: detector and amplifier

The photodetector and readout electronics introduce shot noise and Johnson noise into the measurement, and these must be kept small if the telescope is to reach the photon noise

limit. At an early stage in the design we compared detectors then available - photomultipliers, phototransistors and photofets - and concluded that a photomultiplier was the only choice.

One defect of photomultipliers, already noticed, is their low quantum efficiency (5% to 15%). By contrast some solid state detectors now available, notably Si PIN diodes, have quantum efficiencies as high as 60%. The feasibility of applying a Si PIN detector to our telescope has been investigated recently by R.B. Emmons and S.B. Grossman[16] of Lockheed. The result depends on operating temperature. At 300K shot noise in the detector would far exceed photon noise, but at 4K it would not, and then the high quantum efficiency of the Si PIN detector would be a boon, capable in principle of reducing the final photon noise limit from 1 marc-s/$Hz^{\frac{1}{2}}$ to 0.3 marc-s/$Hz^{\frac{1}{2}}$. Whether one should go this route remains uncertain. Having a cryogenic telescope makes the use of a cryogenic detector seem natural, but the issue is muddied by the need to chop the light signal in order to get rid of 1/f noise. To develop a satisfactory cryogenic chopper is not easy.

With a photomultiplier one must reckon not only with the intrinsic shot noise but also with Johnson noise from the load resistor; and after that the noise in the readout preamplifier. In our original study we compared noise levels in mV at the input of the preamplifier, scaled to the 20 KΩ load resistor of a 1P21 photomultiplier; here we translate the same results into units of angular noise in marc-s/$Hz^{\frac{1}{2}}$, and add the data derived by Emmons and Grossman for Si PIN detectors. The results are presented in Table 2; they show

Table 2: noise in telescope output for various detectors

		marc-s/$Hz^{\frac{1}{2}}$
photon noise at 5% quantum efficiency	focused diffraction limited optics	1
noise from various photodetectors of 1969 vintage	selected 1P21 photomultiplier	0.7
	selected 4441A photomultiplier	0.5
	phototransistor	2300
	photofet	1600
noise from readout preamplifier	----------	0.01
overall noise performance with Si PIN diode detector of 60% quantum efficiency	at 300K	18
	at 4K	0.3

that photomultipliers or a cooled Si PIN detector will allow the telescope to reach photon noise limit, but that the other detectors are unacceptable.

Sharpness of the image divider

We have seen that displacements of the star image across the dividing edge can give rise to telescope errors because of the nonlinearity of the image. Displacements along the dividing edge may also cause errors if the prisms are chipped, or curved along the roof-line, or are not orthogonal to each other.

These errors were first investigated by R.A. Nidey[17]. To evaluate them we assume that the pointing controller keeps the telescope within a range θ_p in each axis, and then ask what effect a mispointing of θ_p in one axis has on the readout in the other. Errors from roof curvature are negligible. To avoid cross-talk from nonorthogonality of the roof-lines, the misalignment ϕ should not exceed Δ/θ_p, where Δ is our 0.1 marc-s criterion, from which with a θ_p of 70 marc-s we find that ϕ should be below 5 arc-min. In practice referencing to the gyro readout is likely to establish a more stringent requirement.

A formula for the effects of nicks on the prism edge, somewhat different from the one originally given by Nidey, may be derived as follows. Note first that with a star-image approximating to a uniformly illuminated disk there is no error so long as the nick lies always inside the disk. Trouble arises only when cross-axis motions of the beam along the roof-line bring new nicks into or out of the image. The worst error comes when an elongated chip of width w deflects light that should have fallen into one half image over into the other half image. The null shift, which has to be less than Δ, is then $\theta_p w/d$, where d is as usual the image diameter, and w and d are expressed in similar units of linear or angular measure. Now θ_p must be less than R, where R is the allowed range of motion across the prism edge given by Equation (4), that is $R = 1.15\ \Delta^{1/3}\ d^{2/3}$. Combining results, eliminating d, and multiplying by focal length f to convert to linear measure, we find for the

maximum acceptable width

$$w < 0.81\ R^{\frac{1}{2}}\ \Delta^{\frac{1}{2}}\ f \qquad \text{defocused image} \qquad (11).$$

With an f of 150 in, an R of 70 marc-s and a Δ of 0.1 marc-s, Equation (11) gives a maximum width of 1.6 μin for chips longer than $2\theta_p f$ or 100 μin. Shorter nicks can be wider; the limit on a square nick, for example, is 13 μin.

The reader may find it peculiar that the criterion of Equation (11) becomes more stringent the smaller the pointing error. Obviously nicks on the prisms would have no effect in a telescope pointed to 0.1 marc-s. Equation (11) is a design criterion, applicable only when $\theta_p >> \Delta$, which implies that if one has enhanced the telescope's linear range by defocusing one can also accept bigger nicks. The basic formula $w<\Delta d/\theta_p$ shows, as expected, that w must decrease as θ_p increases.

Since the limit on w for a long nick, set by Equation (11) with a 1.8 arc-s image, is the exceedingly small number 1.6 μin, one might suppose that the nick criterion provides a real argument in favor of defocusing. Not so. A focused image, being a diffraction pattern, has sloping rather than vertical sides, and as a result the amount of light shifted from one half image to the other when the image moves through an angle $2\theta_p$ is proportional not to $w\theta_p/d$ but to $A\theta_p/d^2$, where A is the area of the nick. The greatest shift occurs in the region of steepest slope of the diffraction curve, i.e. at the Airy radius $0.61\lambda/D$. The Gaussian approximation yields $A\theta_p<\pi^{\frac{1}{2}}d^2\Delta/2$, from which instead of (11) we get the two equivalent formulae

$$\left.\begin{aligned} A &< 1.15\ R^2 f^2 \\ A &< 1.08\ \Delta^{2/3}\ \lambda^{4/3}/D^{4/3} \end{aligned}\right\} \qquad \text{focused image, monochromatic light} \qquad (12)$$

The limiting nick width derived from Equation (12) is much less severe than that from Equation (11). For a square nick w must be less than 58 μin; for a rectangular one 300 μin long it must be less than 11 μin.

The existing prisms have no detectable long nicks above 1 μin, and no short nicks of dimension greater than 5 μin.

Distortion under temperature gradients

A temperature gradient ∇T across an element $d\ell$ of material of expansion coefficient α will distort it through an angle $\overline{d\theta} = \alpha\ \overline{d\ell} \times \nabla T$. Applied to the telescope this means that a transverse heat flux warps the structure, tilting the secondary mirror and producing lateral displacements of it and the image dividers. Both effects shift the null point of the telescope. The distortion is lessened if the telescope is surrounded, as indeed it is, with a sheath of aluminum or other high conductivity material. The null shift may be expressed in terms of the total transverse heat load, assumed for simplicity to be uniformly spread over the projected area of the telescope. A closer investigation will take into account specific sources of heat - for example, the temperature controller of the gyro readout magnetometers. Let the thermal conductivities of the telescope tube and sheath be k and k', and their wall thicknesses be w and w'. Let f and ℓ be the focal length and physical length of the telescope, f_1 the focal length of the primary mirror, and ϕ the angle between the direction of heat flow and the plane of an image divider. Then in the worst case where the sheath and telescope tube are in thermal contact, the null shift arising from a heat load Q is

$$\theta_T = \frac{\pi}{4}\left[\frac{\alpha Q}{kw + k'w'}\right]\frac{f_1}{\ell}\left[\left(1+\frac{\ell}{f}\right) + \frac{\ell}{f}\left(\frac{f}{f_1}-1\right)\right]\sin\phi \qquad (13)$$

from which we find that θ_T for our telescope is $4.17 \times 10^5 \alpha Q/(kw+k'w')$ arc-s, or transposing the result into an upper limit Q_{max} on the transverse heat load with θ_T being kept below 0.1 marc-s, we have $Q_{max} < 2.4 \times 10^{10}(kw+k'w')/\alpha$.

Putting in numerical values for α, k and k', and taking the wall thickness as of the telescope and aluminum sheath as 1 cm and 0.3 cm respectively, we get the results of Table 3.

Table 3: maximum allowable tranverse heat loads (mW) on the telescope at different operating temperatures

	2K	77K	300K
without aluminum sheath	0.05 mW	0.0001 mW	0.0008 mW
with aluminum sheath	11.5 mW	0.03 mW	0.06 mW

Table 3 shows how crucial operation at 2K is, and also how even at 2K care is needed. Consider first a telescope at ambient satellite temperature, sideways on to the sun. The total heat load from the radiation over the projected area of the telescope is 80W. For a telescope with an aluminum sheath the heat load would have to be reduced by a factor of 1.4×10^6; for one without a sheath it would have to be reduced by a factor of 10^8. Even with extremes of insulation, and a rolling spacecraft, these requirements are exceedingly hard to meet.

Now consider a telescope at 2K mounted in a dewar. We must examine sources of heat both internal and external to the dewar. For the latter the allowable transverse heat flux is just the 11.5 mW determined in the presence of the aluminum sheath. The total heat load down the neck of the dewar is 66 mW. Most of this is very symmetrically disposed and is shorted out at heat station 0 of the dewar (see accompanying paper by Parmley, Goodman, Regelbrugge and Yuan[18]). The only direct heat load on the telescope is radiation from the last gold-coated window, which is 0.6 mW, and also very symmetrically disposed. The heat conducted from the leads to the probe support structure is 0.36 mW. A conservative estimate would put the transverse heat flow across the sheathed telescope from these external sources well below 0.1 mW, i.e. at least a factor of 100 below our requirement. The largest internal source of heat is the temperature controller for the gyro readout magnetometer, which may contribute as much as 2 mW. If the controller were attached directly to the telescope/quartz block assembly, it could cause trouble, but being on the probe support structure it has no ill effect.

Thus a low temperature telescope has an absolute stability better than 0.1 marc-s. Errors from this sources are eliminated even without spacecraft roll.

Change in focal length on cooldown

The position of the focal plane of the telescope changes slightly on cooling from room temperature to liquid helium temperatures. The effect was first investigated by R. Woodruff[19] of Ball Aerospace. It causes an image shift along the axis given by

$$\partial = \bar{\alpha}\ell \left(\frac{2f_2 f_1 + 3f_1 \ell - 3\ell^2 - 6f_2 \ell}{f_2 f_1 + f_1 \ell - \ell^2 - 2f_2 \ell} \right) (T - T_o) \qquad (14)$$

where $\bar{\alpha}$ is the mean coefficient of expansion between T and T_o. The net shift is about 1.3 mil. With an image which at room temperature is precisely in focus the effect of cooldown will be to defocus it slightly, increasing the diameter by about 10%.

Null shifts from tilt or unequal heating of the dewar windows

Before the starlight enters the telescope it passes through three gold-coated windows, placed in the dewar neck to lessen radiative heat loads into the probe assembly. The windows are optical flats, made from either fused quartz or sapphire of Schlierren quality, of aperture 7 in and thickness 0.5 in, polished flat to $\lambda/20$ and parallel to 0.5 arc-s. They operate, as indicated in the accompanying paper by Parmley, Goodman, Regelbrugge and Yuan, at temperatures ranging from 40K for the coldest to 150K for the warmest. The residual aparallelism makes each window deflect the star image from its true direction by some 250 marc-s; however, provided there is no other change, this deflection, being constant, has no ill effect. We now examine whether there can be any time varying contributions to the deflection - through, for example, a change in tilt of the window or a changing temperature gradient across it in the direction at right angles to the line of sight to the star.

When a uniform block of glass with truly parallel faces, placed in a parallel beam of light, is tilted through a small angle it shifts the beam sideways but does not change its direction. Only if the block is wedge-shaped will there be a deflection. Let the wedge angle be β, assumed to be small. Then the greatest allowable change $\delta\psi$ of tilt is given by

$$\delta\psi < \left[2\frac{\Delta}{\beta} \left(\frac{n}{n^2-1} \right) \right]^{\frac{1}{2}} \qquad (15)$$

where n is the refractive index of the window, and Δ is our 0.1 marc-s stability criterion. With a β of 0.5 arc-s, the maximum allowable change of tilt is 1.2° - far in excess of anything that will in fact be encountered. Tilt is not an issue.

The case is far otherwise with temperature gradients. Here we must consider effects of both thermal expansion (which with a transverse gradient changes the window from a flat to a wedge) and changes in refractive index with temperature. With a window of aperture D and thickness ℓ, having a temperature difference ΔT across its diameter, the displacement θ_T of the line of sight is

$$\theta'_T = \frac{\ell}{D}\left[(n-1)\alpha + \frac{dn}{dT}\right]\Delta T \qquad (16)$$

where α is the expansion coefficient and n is again the refractive index. The two terms in Equation (16) tend to balance out - when α is positive dn/dT is negative, and vice versa - but not completely. Usually dn/dT is about twice $(n-1)\alpha$. For a quartz window at 150K the temperature difference ΔT has to be less than 40mK to keep θ'_T below our design limit Δ of 0.1 marc-s.

Such a small transverse temperature gradient may not be easy to come by. As usual our ultimate concern is with the roll-averaged effect, but we start by considering the absolute effect, with a quartz window the transverse heat flow would have to be kept below about 0.1 mW, which is very small in comparison with the total amount of heat impinging on the first window from above (roughly 1 W). A gold coating on the window, facing outward, would ease the difficulty, but even with 90% reflectance the load is still 100 mW. Asymmetries large enough to cause null shifts are easy to imagine. Uneven heating by black body radiation from the walls of the sunshade in front of the telescope are one example; effects from the earth's albedo are another. The latter originate in the portion of the orbit when the star is occulted by the earth, but owing to the long thermal time constant of quartz (>500s in the transverse direction for a window at 150 K) they tend to persist into the observation period. The best solution to both difficulties may be to use a sapphire window. Sapphire does not absorb the infrared as well as quartz, but its thermal conductivity at 150 K is a factor of 200 higher.

Besides the potential for null shifts from a nonuniform heat load, there is the effect of a uniform load in converting a flat window to a lens through the difference in temperature between the center of the window and its edge. The difference for a quartz window at 150 K carrying a load of 1 W is of order 5 K. Assuming symmetry and a uniform flux Φ_o over the surface, the focal length f of the lens created from a uniform window of refractive index is

$$\frac{1}{f} = \frac{\Phi_o}{2nk}\left[(n-1)\alpha + \frac{\partial n}{\partial T}\right] \qquad (17)$$

which turns out for our window to be of order 20 km - of no significance to the telescope's performance.

Summary

The calculations just given, along with the results presented earlier in the section on rationale, indicate that a telescope of the proposed design will have the requisite mechanical and optical stability. It will also be adequately linear. With focused optics the intrinsic linearity of the image will be 0.1 marc-s over a range of ±33 marc-s, or 0.5 marc-s over ±50 marc-s. A wider range may be had by any of three methods: apodizing the telescope aperture, defocusing the image slightly, or compensating electronically for the cubic term in the transfer function. A 50% increase in image diameter through defocusing is probably allowable; it would extend the range over which the signal has 0.1 marc-s linearity from ±33 marc-s to ±43 marc-s. Electronic compensation, properly applied with good optics, might extend it to ±70 marc-s.

To prevent null offsets in the telescope readout through cross axis motions of the image, a limit must be set on the dimensions of any nicks on the sharp edge of the image divider. Taking the worst case where there are prolonged periods in which the telescope is mispointed through an angle θ_p comparable with its limiting range R, one finds that with a focused image the maximum acceptable dimension for a square nick is 58 μin. Progressive defocusing has the effect first of imposing a more stringent requirement and then of gradually relaxing it again. With an image defocused to a diameter 50% greater than that of the Airy disk, the requirement would be only slightly more stringent than with a focused image.

Great care must be taken to make sure that there is no temperature difference of more than 40 mK across the diameter of the first gold-coated radiation window in the dewar neck.

With Rigel as the guide star, and a 4441A photomultiplier operated at a chopping frequency of 50 Hz as the detector, the expected noise performance of the telescope is 1 marc-s in a 1 Hz bandwidth or 3 marc-s in a 10 Hz bandwidth as stated in Table 1.

Design and fabrication of the optics

Having established the basic design concepts and equations we were able to proceed to detailed design and the fabrication of the optics. Once the physical dimensions had been established, the limits on aperture and focal length defined themselves. Our reasons for choosing a three mirror system have already been explained. Initially our desire for a long focal length sprang from concern over the difficulty of making roof prisms with edges sharp enough to meet the requirement of Equation (11). Recognizing that in fact the correct requirement is the less stringent one of Equation (12) one might now argue for a shorter focal length, and indeed in the flight design a reduction of f from 150 in to say 120 in may be reasonable. Too short a focal length would still be a mistake.

Design and fabrication for the most part followed established optical procedures, adapted

in some places to make the structure suitable for assembly by optical contacting. The following subsections cover the principal points.

Optical layout

The optical layout was developed by a ray-tracing program, subject to practical constraints on the fabrication of the three mirrors and the corrector plate. With manufacturing tolerances of $\lambda/10$ a design based on spherical surfaces and a corrector plate was strongly to be preferred over any attempt to work with aspheric surfaces. The remaining practical concerns were the figure of the corrector plate and the difficulty of making small mirrors without degrading the performance through rounding of the mirror edge.

The corrector plate has to be figured in such a way that one does not run of glass; the manufacturing procedure must leave a flat central region to which the image dividers and light box can be contacted, and a flat outer region to which the 45° exit mirrors can be contacted. Preferably also the correction will be small, for the larger the correction the harder will it be to work the surface to the proper shape. Critical factors are the diameter of the secondary mirror and the location of the "neutral zone", that is, the region of the corrector where the curve has a minimum and light is transmitted without deflection.

Practical experience on the part of one of us (D.E.D.) strongly suggested that the neutral zone should have a diameter about 0.85 times the telescope aperture D. The diameter chosen for the secondary affects the amount of the correction, besides fixing the diameter of the central obscuration and thus of the space in which the light box must fit. Picking first a trial focal length for the primary mirror and trial diameters for the neutral zone (0.85D) and the secondary mirror (0.5D), one can trace rays through the neutral zone to determine curvatures for the secondary and tertiary mirrors, and an approximate diameter for the tertiary. With the mirror curvatures established one next traces rays over the rest of the aperture to get the correction curve for this prescription, after which one can iteratively vary the prescription until one arrives at a design having an acceptable diameter for the secondary, and minimal correction.

Final mirror curvatures were: primary -46 in, secondary +70.050 in, tertiary +7.917 in. The diameter of the secondary came out at 0.458D or 2.59 in. A pleasant unforeseen consequence of having the third mirror was that the correction for it tends to compensate those for the first two, making the net correction substantially less than it would have been in a conventional Cassegrainian telescope. The maximum correction is, as Figure 1 indicates, 31 μin or three fringes.

A consequence of having the large central obscuration, accepted from the beginning, is that more light is thrown into the first diffraction ring than is usual in telescope imaging. This modifies the linearity but not in a deleterious way. The resultant linearity is represented, as discussed earlier, by the range-error relationship of Figure 3.

In 1984 R Sigler[20] of Lockheed Palo Alto Research Laboratory applied Lockheed's ACOSS-V telescope computer optimization program to a further study of the present telescope design. According to his investigation the geometric spot diameter in our layout is about 80% of the Airy disk diameter. A modest redesign with different mirror curvatures and a stronger correction (five fringes instead of three) would reduce the geometric spot by a factor of three to four and might also slightly improve the telescope linearity. Dr. Sigler investigated other matters also, for example, centering requirements. Final design choices here, as elsewhere, involve a combination of analytical and practical considerations.

Design of telescope tube

Since the telescope is made to operate in an evacuated chamber, pump out holes have to be provided in the support tube and light-box assembly, so that the pressures will be the same inside and outside. The holes are sufficiently large and in the right places to be of use also in cleaning the optics and attaching extra light baffles without taking the contacted joints apart.

The tube was of drawn quartz, as a result of which it had some porosity and was in consequence hard to polish to the degree needed for making trustworthy contacted joints to the telescope's baseplate and corrector plate. Although we did succeed in producing joints that have lasted fifteen years we decided that for the shake test model described below we would change the approach by fusing rings of clear fused quartz to each end before polishing and assembly.

To preserve alignment the ends of the tube were polished flat and parallel to within 2 arc-s.

Design and fabrication of the image dividers and beam-splitter

Our reason for employing fixed image dividers, rather than a vibrating reed or rotating knife edge, has already been explained. Having reached that decision our first thought was to split the star on a pyramid, but the sharpness requirement soon ruled out that idea. To fabricate a pyramid with a point sharp to 12 or even 60 μin seems well-nigh impossible. Roof-prisms are easier. Thus we were driven to the idea of two star images and a pair of image dividers. We chose roof prisms as the best method then available, though other methods of making a sharp edge might now be considered - cutting a line on a sputtered film, for example, by photolithography or an excimer laser. Even today, as it turns out, the roof prism would still seem to offer the sharpest edge.

The prisms were made and checked in the following way. First two rough cubes of fused quartz (side 1 in)were polished flat on one face and optically contacted together with provision for separating them later on. Then a second polished cut was taken across the two joined blocks, accurately at right angles to the first. In this way two roofs were formed, with each prism protecting the other's edge. The parts were separated and the edges checked for nicks, first by means of a scanning electron microscope and then by an optical technique due to W. Angele[21] in which the prism edge was illuminated from the side and the observer looked for the diffraction haloes from light scattered from the nicks. The resolution of the electron microscope was such as to establish that the prisms had long sections with no nicks more than 5 μin across, an order of magnitude smaller than the limit set by Equation (11). The optical method is more qualitative but has the merit that it can be applied to check the prisms in situ during telescope assembly.

To get two star images one needs a beam splitter. This constituted a difficult part of the design. Conventional beam splitters are made from two 45° prisms cemented together with a half-silvered interface. Ours had to be made without cements in order to ensure mechanical stability and remove the danger of its coming apart while being cycled to low temperatures. We used a half-silvered plate tilted at 45° and optically contacted to a base-block. Trouble from the resulting astigmatism in the transmitted image was averted, as mentioned earlier, by using that image for the readout axis in which the astigmatism was parallel to the roof line.

Acquisition range and the dimension of the light pipes

An important point in telescope design is the acquisition range. Various procedures may be devised for capturing the guide star, but all depend on providing approximate pointing by some instrument external to the cryogenic environment, and then performing the last stage of acquisition by the telescope itself. In the acquisition process the telescope does not have to explicitly measure the misalignment angle. What it must do is provide a signal for use as a command to the pointing controller, so that the spacecraft will start turning in the right direction to bring the star eventually into the region of the telescope's linear response. The range must be wide enough to cover the greatest expected misalignment between the null directions of the telescope and the external reference instrument, say 1 arc-min. This consideration fixes the diameter of the light pipes. With a 150 in focal length telescope, a 1/8 in diameter light pipe, which was the size we chose, yields an acquisition range in each axis of ±1.4 arc-min. The 2 arc-min range specified in Table 1 would require a 3/16 in pipe.

Assembly and alignment of the telescope parts

The overall plan of the experiment requires that the null points of the gyro and telescope readouts be within 5 arc-s of each other (Table 1). This in turn requires the optic axis of the telescope to be normal to the under surface of its baseplate to within 2 arc-s. Alignment proceeded in five phases as follows:

First, the primary and tertiary mirrors were contacted to the baseplate, the telescope tube was also contacted to the baseplate, and the secondary mirror was contacted to the lower (flat) face of the corrector plate. The critical issue here was centering. The mirrors had been made by first lapping and polishing the optical surfaces, and then setting up each piece on a rotary grinder to form its outer edge and, for the primary and secondary mirrors, the center holes also. Optical tests and adjustments during set up made the optical and mechanical centers coincide in each case to within about 0.5 mil. The curve in the corrector plate was centered to a like precision. The edges and center holes then provide the reference surfaces for assembly, starting with the contacting of the primary mirror to the baseplate. The tertiary mirror was centered in the hole of the primary with the help of a conical sleeve of aluminum, and then pressed into contact. The overall error in centering of the optics axes for the two mirrors, allowing for the uncertainties in fabrication and assembly, was probably under 1 mil. Centering of the telescope tube was less critical and was done by eye. Centering of the secondary mirror on the corrector plate was by reference to the holes in the mirror and plate and was again good to 1 mil or

better.

The second phase of alignment was to mount the corrector plate on the telescope tube. First three 1 in X 2 in X 4 in pyrex blocks were contacted temporarily to the underside of the baseplate, so that a portion of each block extended out about 1½ in from the edge of the plate. These blocks served as reference surfaces to establish the plane of the baseplate as seen from the entrance to the telescope. Next the telescope was stood upright on the granite table, resting on the three pyrex blocks; the corrector plate with the secondary mirror was set on top of the telescope tube; and a Davidson Optronics Model D638 5 in aperture star-autocollimator was supported vertically downwards over the telescope, sharing aperture with the telescope and one of the pyrex blocks, so that half the beam was reflected from the block while the other half passed through the telescope and came to a focus just above the corrector plate. The light-beam was aligned normal to the pyrex block to within the limit of the autocollimator adjustment, that is to within 0.1 - 0.2 arc-s. The corrector plate and secondary mirror assembly was then positioned until the focused beam from the autocollimator came out centered on the hole in the corrector plate. Finally the plate was contacted to the telescope tube, with centering that we deem again to have been good to better than 1 mil.

The third phase consisted in finding the focal planes. With the autocollimator still in position, the beamsplitter, which had already been contacted to the support block, was contacted to the corrector plate, using the light from the autocollimator as a centering reference. Next the telescope was laid on V blocks on the corrector plate fixture, and with the aid of a pinhole and knife edge at the focal plane was adjusted to autocollimate off a 6 in diameter optical flat mounted normal to the telescope axis. The observer stood at the side of the telescope, viewing the image through a right angle prism, and adjusted the position of the knife-edge/pinhole assembly until a uniform cut-off was seen over the whole aperture. This was the focal position. The distance from the pinhole to the corrector plate was then carefully measured, and with that distance known, it became possible to settle on the proper height for the light box. This involved measuring the height of the upper roof prism with a travelling microscope and cutting the light box to a dimension that would put the edge of the prism at the focal point of the transmitted light.

With the parts appropriately dimensioned it was possible to proceed to the fourth phase of alignment: assembly of the prisms and light box. For this purpose the star-autocollimator was again set up to look simultaneously at light reflected from the pyrex block and light transmitted through the telescope optics, but now a special feature of the D638 star-autocollimator came into play, a built in eyepiece that allows one to observe simultaneously three things: (i) the pinhole for the light source, (ii) the image of the pinhole autocollimated through the telescope, (iii) the image of the roof-prism on which the star-image is supposed to fall. When the alignment is correct all three should coincide and be in focus.

The prism on the corrector plate was aligned first. First that autocollimator was aligned with the pyrex block to 0.1 - 0.2 arc-s. Next the prism was adjusted until its edge exactly split the star image, the focus was checked by seeing that the image of the prism edge and pinhole were simultaneously sharp, and when both conditions were satisfied the prism was contacted to the corrector plate. A similar procedure was adopted for the second prism. First the light-box was contacted to the corrector plate in the right orientation to make the four output beams emerge through the holes in the side of the box. Next the prism, centered by eye, was contacted to the cover plate for the box. Then the cover plate was placed on the box and moved about until this roof edge also, viewed through the appropriate hole in the box exactly split the star image. Lastly the cover was contacted to the light box.

A final check was to view each roof prism through the eyepiece, adjust the beam until the image was centered and then read off the misalignment angle between the reference block and the autocollimator. The error, measured to the 0.1 - 0.2 arc-s precision of the D638 autocollimator, appeared to be no more than 1 arc-s in each axis.

The fifth and last phase of assembly involved contacting the refocusing lenses to the light-box, and the 45° output mirrors and light-pipe guides to the outer region of the corrector plate. The assembly was checked by placing the telescope in the beam of a large (20 in aperture, 150 in focal length) collimator, whereupon the star images were seen to emerge properly centered on each light-pipe guide.

Figure 4 shows two views of the assembled telescope.

Mechanical integrity of the telescope structure

Optical contacting is an ancient art[22] still not well understood. Since the classic

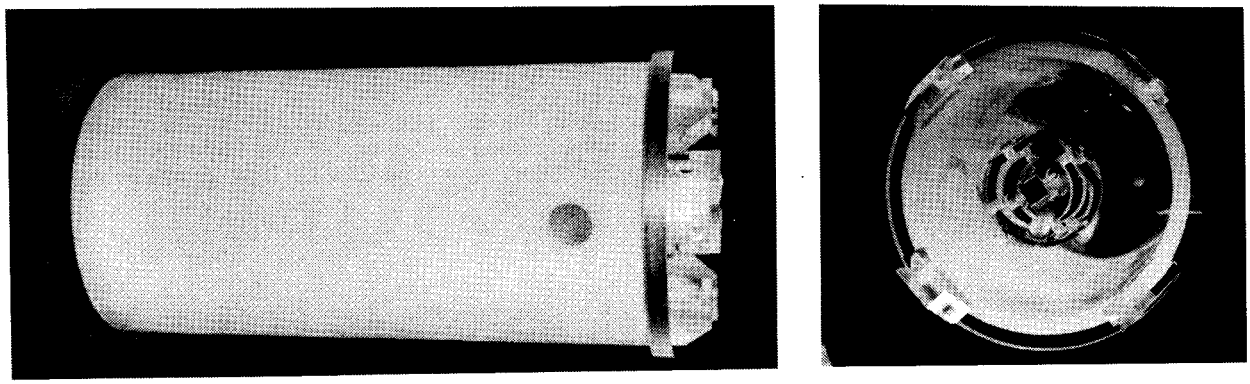

Figure 4: assembled quartz telescope

experiments done in 1935 by the 4th Lord Rayleigh[23], there have been relatively few systematic studies. A recent NASA technical memorandum by J.J. Wright and D.E. Zissa[24], which includes the results of an extensive literature search, lists no more than ten papers on contacting techniques from the period 1964 through 1977.

We report here on certain tests that we and colleagues at NASA Marshall Center have made to investigate whether a telescope of the proposed dimensions, held by optical contacting, will survive low temperature cycling and the vibration of launch. The tests are far from complete. They are of two kinds: specific experiments on optical contacts, and the vibration of a mass model of the telescope. In assessing them it is important to bear in mind that optical contacting works through the surfaces conforming to each other by elastic distortion. A good optical flat, polished to a twentieth of a wavelength, has variations in surface contour of 500Å. When put together two such surfaces will have some regions in contact and some separated by 1000Å. Now the van der Waal's forces which govern the process vary with intersurface distance d as $1/d^4$, and only reach a magnitude corresponding to the ordinary tensile strength of the material when d becomes comparable with the interatomic spacing (5-10 Å). The initial strength of a contacted joint, therefore, will depend on the ability of the two surfaces to conform, and that obviously is greater for thin pieces of glass than for thick ones. We should not blithely assume that tests on thin pieces will be relevant to the strength of the joint between the telescope tube and baseplate, both of which are very stiff. On the other hand, neither should we overlook the possibility of a joint's improving with age. The local stresses created by the van der Waals' forces are so great that surfaces initially in poor contact may eventually conform viscoelastically. In an important paper from 1976, Berthold, Jacobs and Norton[25] have shown that over periods of hundreds of days test pieces made from pairs of fused quartz blocks in contact will progressively shrink by as much as 300Å in the overall dimension normal to the contact - presumably because the two surfaces are slowly pulling each other into conformity.

Tests of optical contacts

A simple test which we performed in 1965 was to form a contacted joint between two fused quartz blocks, each 3/4 in square and about 3/8 in thick, and cycle it many times to liquid nitrogen and liquid helium temperatures. At first we cooled the sample slowly ($\sim$ 1 hour) by enclosing it in an isolation chamber before placing it in the liquid; later we subjected it to the severe shock of dunking it in liquid nitrogen, cooling it more than 200°C in a minute. In no circumstance did the joint come apart. The surface flatnesses of these blocks were not specified but were probably good to about $\lambda/10$ (500Å). Some years later, in 1970, we tested another sample which did come apart when dunked in liquid nitrogen, but upon investigation we discovered that by mistake it had been made of crown glass rather than fused quartz, so we attributed that failure to differential contraction. Crown glass shrinks by at least an order of magnitude more than fused quartz on cooling from 300K to 77K. Another fused quartz sample made later in 1970 from two circular blocks, each of 1 in diameter and finished to the same $\lambda/20$ quality as the primary contacts of the telescope, has withstood pull tests and temperature cycling over a period of fifteen years without failure. Even with fused quartz, however, the reliability of the joints does depend, as noted below, on the details of the contacting procedure.

Application of superfluidity to test intimacy of contact

Having completed the initial test in 1965 we conceived a slightly more sophisticated

experiment to check the intimacy of contacted joints at liquid helium temperatures. We took two 2 in square optical flats, each about 1/2 in thick, one a plain flat, the other having a small cavity in the center of its contacting face, connected to a hole from the other side, ground and tapered to 3°. Upon contacting the two parts formed a little chamber as shown in Figure 5(a). Into the tapered hole we cemented a standard quartz taper fitting, to which had been attached a quartz-to-metal seal and stainless steel pipe, allowing the whole to be immersed in liquid helium and connected to a helium leak detector as shown in Figure 5(b). Three tests were then performed: (i) the contacted chamber was

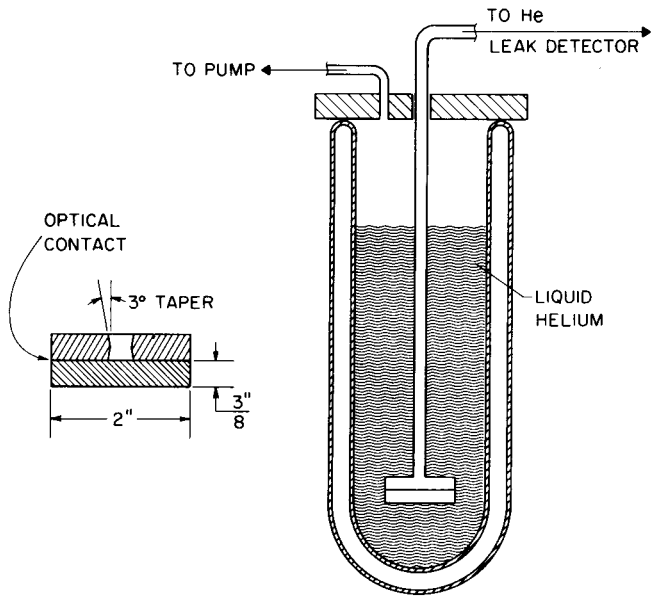

Figure 5: apparatus for testing optically contacted joints at cryogenic temperatures

surrounded by a bag full of helium gas at room temperature, (ii) the chamber was placed in the dewar of Figure 5(b) containing normal liquid helium at a temperature of 4.2K, (iii) the liquid helium was cooled to 1.4K by pumping on the bath, and therefore became superfluid. In no instance did we detect any sign of a flow of helium through the joint even after periods of many minutes accumulation on the most sensitive scale of the leak detector (10^{-9} st.atm.cc/s).

The experiment, especially with the superfluid, offers an extremely powerful test of the closeness of contact. Superfluid has been shown to flow with ease through pores as fine as 20 Å in diameter. Let us examine by simple calculation the limits on the gap set by the measurements with normal and superfluid helium.

With a normal liquid the flow rate is just the volume flow rate $\dot{V}$ times the liquid density ρ_n. Assuming laminar flow, as one should since the Reynolds number will be far below 2000, the mass flow rate between two circular plates of radius r_2, separated by a distance d, and leaving an access port of radius r_1 in the center, is

$$\dot{m}_n = 0.3 \frac{\rho_n}{\eta} d^3 \frac{r_1}{r_2+r_1} P \qquad (18)$$

where η is the viscosity and P the pressure difference between r_1 and r_2. Transposing into a limit on d, and inserting numerical values $\dot{m}_n \sim 5X\ 10^{-13}$ gm/s (10^{-9} st.atm.cc/s of helium), $r_1 = 0.5$ cm, $r_2 = 1.5$ cm, and (for helium at 4.2K) $\rho_n = 0.14$ gm/cc, $\eta = 35 \times 10^{-6}$ poise, $P = 10^6$ dyne/cm (1 atmosphere), we get for the upper limit on d

$$d < 9\ \text{Å} \qquad (19)$$

The calculation is, of course, oversimplified in that close to r_1 there will be transitions in the gap from liquid to gas, and from dense to rarefied gas. The effect of the corrections is minor, however. Also the estimated d is conservatively large, because in estimating $\dot{m}_n$ we have made no allowance for the increase in effective sensitivity of the leak detector that comes through using the accumulation technique.

With superfluid the only limitation on flow (save for a proviso to be discussed in a moment) is the critical velocity v_c of the liquid. The mass flow rate is

$$\dot{m}_s = \rho_s v_c A = 2\pi\rho_s r_1 (v_c d) \qquad (\ )$$

where ρ_s is the superfluid density. Critical velocities vary as a function of the gap d, with the product $(v_c d)$ being essentially constant over a certain range of d. Setting v_c arbitrarily at 100 cm/s, its value for a d of 100 Å, we get the preposterously inconsistent limit on d of 10^{-6} Å. We are evidently well into the range where superfluid flow is impossible; our best estimate is

$$d << 10 \text{ Å} \qquad (\ )$$

Thus the tests in liquid helium, both normal and superfluid, strikingly confirm the intimacy of optical contact.

The superfluid measurement has one potential flaw. In any low temperature apparatus where an open pipe leads from room temperature to the experiment chamber, thermal radiation coming down the pipe supplies heat to the chamber. Absent any baffles, enough heat may have entered the inner region of the contacted joint in our apparatus to warm it above the superfluid transition temperature (2.16K). In such a situation the helium would have been converted from superfluid to normal fluid at some radius r_3 between r_1 and r_2. The flow rate would then be controlled by the viscosity of the normal fluid, and to find the limit on d one would have to fall back on Equation (18) with the unknown r_3 substituted for r_2. The limit would in any case be smaller than the 9 Å set by (19). The transition to normal fluid is possible despite the nominally infinite thermal conductivity of superfluid helium, because the amount of heat which the creeping film can transport is limited, especially in narrow gaps where the normal fluid is constrained. It would be interesting to repeat the experiment with proper radiation baffling.

Pull tests on contacted joints at room temperature and low temerature, performed at NASA Marshall Center

Another series of tests, initiated at NASA Marshall Center by W. Angele and P.L.Peters, were on the strengths of contacted joints. Two apparatuses for making pull tests were developed, one of which could be operated down to liquid helium temperatures. The smaples were mostly disks, 1 in in diameter and 1/2 in thick. Early experiments at room temperature on specimens with different surface flatnesses ranging from $\lambda/2$ to $\lambda/20$, had the rather surprising outcome that within this range strength and flatness had little to do with each other. The pull strength in most instances was about 200 lb/in^2, as compared with the 2000 lb/in^2 tensile strengths typical of solid fused quartz in similar circumstances. Cooling the joints in liquid helium temperatures had two very different effects. Some, which had apparently not been properly contacted, came apart; others, rather surprisingly became stronger. Typical pull strength were 600 to 800 lb/in^2, three to four times the room temperature value. One joint was so strong that even at the limit of the instrument (1300 lb/in^2 for this sample) it still held.

This work, most of which was done by P.L. Peters and L.L. Payne, is briefly described in the report by Wright and Zissa[24]. More details are given in an unpublished document by Payne.[26]

"False contact" and the separation of contacted joints by penetrating oil

A standard test of good contact is the absence of reflections and interference fringes from the joint when it is illuminated by monochromatic light. If moisture is present, however, the test can mislead. In humid weather joints often seem to go together easily, only to produce what is known as "false contact", where the joint passes optical tests but is not truly down. False contacts can be twisted by hand - sometimes only a second of arc- and moved by heavy pressure. There seem to be two reasons for this deceptive ease of contacting on humid days. First, dust is not so attracted to the surfaces; second the forces are acting at a liquid rather than a solid interface.

Effects of moisture seem to explain some intriguing observations made at NASA Marshall Center in 1972 by T.L. Barber[27] and others. Several joints apparently in good contact came apart on being soaked in penetrating oil. This discovery led one of us (D.E.D.) to study the reliability of joints made under different conditions between a pair of $\lambda/20$ flats of diameter 1 3/8 in and thickness 1 in. First the flats were contacted together, subjected to a pull test - which they survived - and then after one hour immersed in penetrating oil. Fifteen hours later the oil had penetrated the joint, and the surfaces were easily slid apart. When, however, the same parts were recontacted and put in an oven

at 250°C for 66 hours before the test, the oil did not penetrate and the joint held perfectly. Our assumption is that heating drives the air and water out of the joint, and that some time is needed for the process to be effective. Ghita and Ghita[20] have reported independent experience on the hardening of fused quartz contacts by heat, also in 1972.

Other experiments have shown that parts placed in a vacuum tank for coating, after having been contacted, come out stronger than before.

Vibration test of the telescope mass model

The successful fabrication of the laboratory telescope gives some assurance that optical contacting can be applied to a flight telescope, but leaves various concerns, especially about the joint between the telescope tube and baseplate. Both parts are, as remarked above, very stiff and may not bond well. An alternative procedure might be "fritting", a technique akin to soldering,in which a powder of lower melting point glass is melted into the joint, typically at about 950°C,just below the annealing temperature of fused quartz. A fritted joint would be strong and stable but might cause other problems. Thus, if the primary and tertiary mirrors as well as the tube were fritted to the baseplate, the heating might distort their figure; alternatively if they were contacted, the contacting would presumably have to be done after the tube was in place, and that would not be easy.

In 1980 we decided to investigate these issues by building a telescope mass model. The model, illustrated in Figure 6, was double ended with fritted joints at one end and contacted at the other. The tubes were of 6 in outer diameter and 1/2 in wall thickness, and thus not

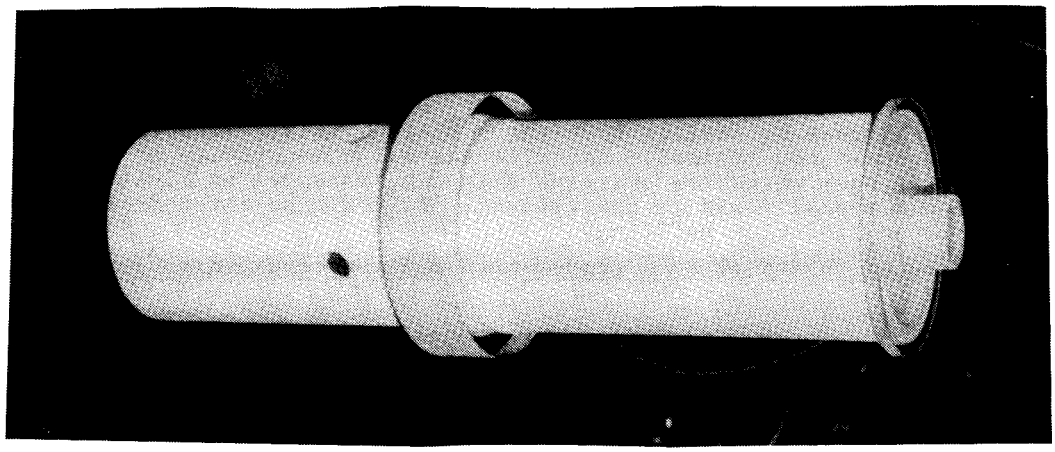

Figure 6: telescope mass model for vibration testing

quite identical with the expected dimensions of the flight telescope (7½ in outer diameter and 3/8 in wall thickness) but close enough for our purpose. The base was an 8¼ in diameter 2 in thick flat plate.

The fritted half had, in addition to the telescope tube, an optical flat, also fritted in position, representing the primary mirror. Its front surface had supposedly been polished to $\lambda/10$ before assembly with the idea of testing the effect of the fritting process on the figure of the mirror. To aid the flow of fritting compound a network of grooves, with 1/2 in spacing, had been cut into the rear surface before the front face was polished. Fritting was performed in the Technical Products Division of the Corning Glass Company under the direction of Donald Baker, and went smoothly. However,through a regrettable oversight we failed to check the flatness of the mirror before the joint was made. The measured flatness afterwards was better than a wavelength but not as good as the nominal $\lambda/10$ - whether because of a change or because of deficiencies in the original polishing remains unknown.

The contacted side had no mirror but had instead a 7½ in diameter, 3/8 in thick plate contacted to the upper end of the tube, representing the corrector plate, and a 2 in diameter, 1 in thick disk contacted to the center of the plate, representing the light box. In making the two contacts off the ends of the telescope tube we followed a different procedure from that used for the laboratory telescope. Instead of the drawn quartz tube with its troublesome porosity we took a tube of cast quartz and had two rings of clear fused quartz fritted to its ends to provide good surfaces for polishing. The finishes of the baseplate, light box fixture and corrector plate were true to $\lambda/20$. Our aim was to finish the ends of the telescope tube to the same quality, but since these end surfaces are difficult both to polish and to measure, they may only have been at $\lambda/10$.

The parts were shipped to NASA Marshall Center in 1981 for preliminary tests prior to contacting and acoustic vibration tests. Contacting was performed by one of us (D.E.D.), after which the completed test model was placed vertically in an oven at 280°F for four weeks to harden the joints. It was then removed for assembly into the Marshall Center acoustic vibration facility to simulate the stresses encountered during shuttle launch. For this purpose it had to be held in a mounting fixture. Our original intention had been to grip the 8¼ in diameter baseplate between two equal and opposed rings with compressive loads normal to the faces of the plate. For various reasons another scheme was adopted in which the plate was gripped radially by a 2 in wide metal split ring around its circumference. As the ring was being tightened, a few minutes after the model had been turned horizontal, the optical contact between the baseplate and the 6 in telescope tube failed and the tube became detached. Thus the acoustic test on the optically contacted half of the telescope model had to be aborted. The fritted joint was vibrated to shuttle qualification levels in planes parallel and perpendicular to the axis and survived perfectly.

The failure of the optical contact would appear to have been consequence of the method of gripping the baseplate.[29] When radial compressive loads are applied to the plate it will tend to bow upwards, greatly stressing the joint from the outside in. Further tests of the mounting method are required as well as acoustic vibration tests of the contacted model. One outcome worth noting is that when the joint to the baseplate failed, the tube and attachments dropped 3 in and the joint to the corrector plate suffered a severe shock. It survived.

Summary

More work is needed on optical contacting; the following are salient points from the work done so far:

. contacted joints between fused quartz pieces survive cycling to low temperature, and even become stronger at low temperature.

. measured pull strength at low temperature are in the range 500 to 800 lb/in^2 (about 40% of the tensile strength of solid quartz), with occasional higher values.

. "false contact" must be avoided.

. joints become stronger as they age, after they have been placed in a vacuum, and especially after they have been subjected to prolonged heating at temperatures a little above the boiling point of water.

. fixtures to hold contacted pieces must be designed not to stress the joints.

. properly contacted joints are so close that they are impervious to superfluid helium.

Testing the telescope

Testing of the telescope proceeded in two stages. First, as mentioned earlier, we used a telescope simulator, comprising a model telescope and artificial star, in order to gain experience on noise and linearity problems and test different chopper-detector assemblies. The simulator was set up initially at the Davidson Optronics plant in West Covina, California and later transfered to Stanford. Next, having built the telescope proper, we designed built and installed at Stanford a full scale star/collimator unit to test it, and performed noise and linearity measurements on the telescope at room temperature. Most of the latter experiments were done by G.J. Siddall and J.T. Anderson. We have not yet tested the telescope at cryogenic temperatures.

To calibrate the artificial stars, both the preliminary model and the final version, we made use of a stellar photometer: a small telescope of 20 in focal length, 2.5 in aperture and 16% optical efficiency, having an eyepiece for viewing the star in reflection from a mirror near the focus, and a photomultiplier to measure the intensity of the focused beam via a slot in the mirror. The photometer under given operating conditions provided a (non-absolute) measure of star intensity, after which, keeping the same sensitivity it could be applied to the artificial star.

The artificial stars each consisted of a pinhole illuminated by a lamp, with suitable optics to provide a parallel beam of light, the direction of which could be varied by means of tipping plates in the diverging beam. Different star intensities were simulated by adjusting the lamp voltages. The change in lamp voltage altered the color temperature of the simulated star, but at the accuracy levels we were aiming at the resultant error could be ignored or corrected for. Another practical limitation of the artificial stars was in image diameter. Since the pinholes had finite diameter, they created geometric

images which in some instances were considerablly larger than the Airy disk of the telescope under test. Thus with the telescope simulator we used 0.5 mil and 4 mil pinholes, which with the 60 in focal length employed in most of the tests gave geometric images of 1.7 and 13.7 arc-s diameter as compared with the 2.2 arc-s diameter Airy disk. With the final star/collimator unit we used 1.0 mil and 4 mil pinholes, which with a 200 in focal length gave geometric images of 1.0 and 4.2 arc-s diameter, as compared with the 0.94 arc-s diameter Airy disk. Obviously the smaller the pinhole and longer the focal length the fainter will be the star. Since there is a limit on the temperature of the lamp compromises have to be made, and it may be necessary to do linearity measurements with a small pinhole and noise measurements with a larger one, and even then apply corrections to the noise measurements for color temperature and defocusing.

Since the artificial star is calibrated from ground based observations, a correction has to be made for light losses in the earth's atmosphere. The calibration applied to the telescope simulator was from measurements made in the mountains behind West Covina, where smog losses were considerable, and the correction was based partly on guesswork. The observations applied in calibrating the final star/collimator unit were performed by G.J. Siddall and C.W.F. Everitt with the photometer attached to the drive for the Crossley 36 in reflector at Lick observatory. They are most trustworthy.

Measurements with the telescope simulator

The telescope simulator, made from parts of two standard Davidson autocollimators suitably modified, was set up on an iron beam about 6 ft long and 5 in square channel cross-section. The telescope had 20 in focal length and 2.5 in aperture; the star in its final form was, as just remarked, of 60 in focal length and 2.5 in aperture. A tipping plate in the diverging beam of the star allowed displacements of the image over a range ±6 arc-s in the horizontal plane, the dial being calibrated in units of 0.01 arc-s. The system was carefully shielded against stray light. In focus the image had a diameter of about 4 arc-s from the combination of pinhole size and diffraction; it could be defocused by moving the chopper-detector assembly, with a displacement from focus of 23 mil giving a 20 arc-s diameter geometric image.

Calibration of the original chopper-detector assembly by two different methods led to the disappointing discovery that only 0.45% of the light entering the telescope reached the detector. Measurements on the 1 ft long light-pipes by themselves disclosed that they had optical efficiencies of 80 to 90%. Eventually it became obvious that nearly all the loss occurred where the light left the light pipe and entered the chopper-detector assembly, so after various tests we redesigned the chopper-detector to the form illustrated above in Figure 2, eliminating lenses and shortening the distance between the photomultiplier and the exit surface of the light pipes. In experiments at Stanford in May 1972 we found that with careful adjustment the optical efficiency of the new assembly could be made as high as 20%, not as good as we would have wished but a decided improvement on the original 0.45%. We still do not understand the cause of all the light losses.

We took date on the linearity of the model telescope with different degrees of defocusing and found as expected that defocusing improves linearity. Results are presented elsewhere,[30] We also investigated the effects of disk and barrel shaped obscurations in the aperture of the defocused telescope. The results of noise measurements at different degrees of defocusing, obtained with the original low efficiency chopper-detector assembly, are reproduced in Figure 7, and compared with the expected photon noise calculated from the known intensity of the reference star using an optical efficiency of 0.45% and a quantum efficiency of 12%. The agreement is surprisingly good, probably fortuitously so. The residual noise of the photomultiplier with the star lamp extinguished was about 10% of the observed noise for Procyon. With a more efficient optical system the percentage would have been even smaller. The noise due to the transistor amplifier alone was negligible.

In performing the linearity measurements we made zero checks between each measurement, because even under quiet conditions there were null drifts as large as 1 arc-s in periods of a few minutes. Experiments like these bring home to one, as no calculation can, the realities of small fractions of an arc-s.

Star/collimator unit (north star simulator)

The star/collimator unit, also sometimes called the north star simulator, was designed to fulfill two functions: (i) testing the linearity and noise performance of the telescope, (ii) as a precision stable reference for gyro testing. The instrument provides a beam of collimated light aimed downwards at an angle of 37° 41' from the horizontal (the latitude of Stanford) and aligned with the earth's polar axis, thus simulating a star at the north celestial pole. For telescope testing it is operated as an artificial star with certain modulating attachments described below. In cryogenic tests the telescope is mounted in a tilted dewar at floor level; in room temperature tests it is mounted in a cradle bolted to

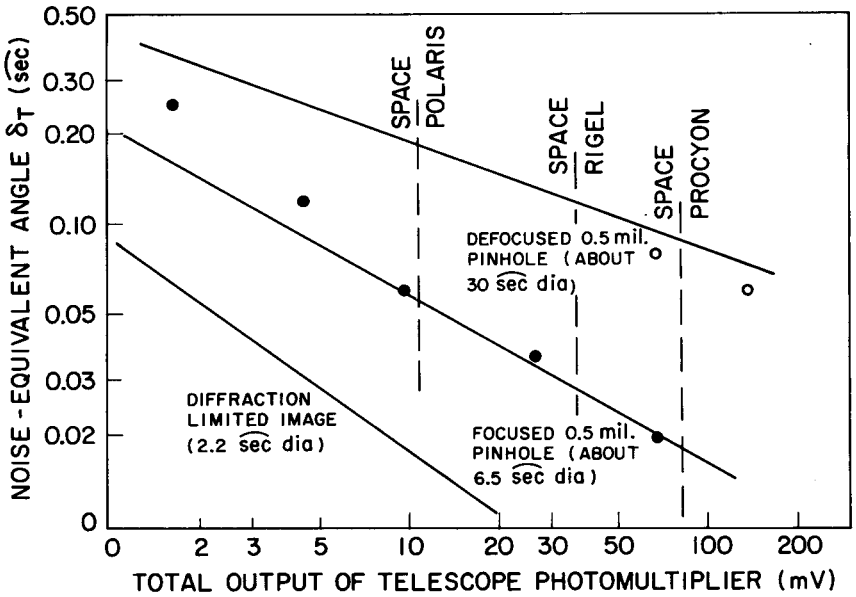

Figure 7: comparison of calculated and measured noise performance for different star intensities in measurements with a 2.5 in aperture telescope and the preliminary chopper-detector assembly

the exit window of the star/collimator unit. For gyro testing the star/collimator unit may be operated either as an automatic autocollimator looking at a mirror on the upper surface of the quartz block or alternatively as a star for use in integrated system tests with the telescope attached to the quartz block.

Figure 8 (a) and (b) give a cross-section (b) and overall view (a) of the assembled unit. It weighs 700 lb and stands 11 ft above the concrete pad on which it is mounted. Its base is an aluminum plate, 2 ft in diameter held approximately 3 in above the concrete isolation

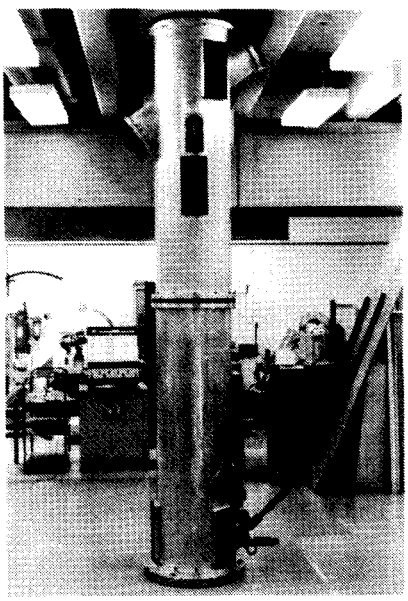

(a) assembled instrument

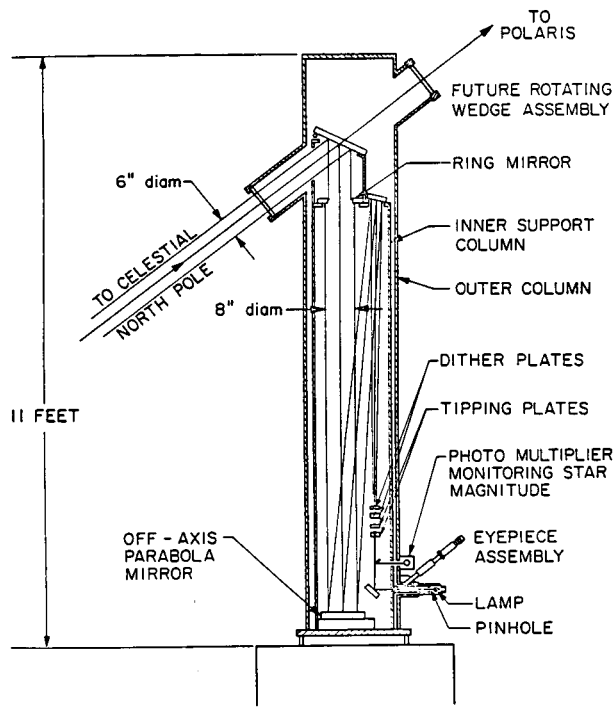

(b) cross-section

Figure 8: star/collimator unit

block by three 1 in diameter steel bolts, with nuts above and below the baseplate allowing it to be levelled. Tangent screws are provided in a housing also fastened to the concrete to adjust the entire instrument in azimuth. The reflection optics and the pinhole of the collimator are all supported on a 16 in diameter aluminum tube, of 1/4 in wall thickness, bolted to the baseplate. Surrounding the inner support tube is an 18 in diameter vacuum tight housing, also of aluminum, with hermetically sealed windows and flanged openings for various pieces of equipment extending inside. Provision is made for vacuum attachments to a forepump to maintain the pressure below 10^{-3} torr. This arrangement,in which the principal optical components are supported on a column inside a vacuum tank,guards the optics from air currents and all but eliminates thermal distortion of the support column from sources of heat in the laboratory. Opportunity has been taken to use the outer tube as an independent support for several devices whose slight motion will not significantly affect the alignment of the autocollimator.

The primary mirror is an off-axis paraboloid set facing upward on the baseplate. The light path is folded twice in the diverging bundle and once in the parallel bundle. An 8 in diameter clear aperture beam passes vertically upwards from the off-axis parabola to an inclined mirror on top of the inner column where it is reflected into the dewar at the proper latitude angle. A mechanism is provided by which the mirror can be swung out of the way, leaving a clear line to Polaris through the exit window of the collimator and a second port on the far side, to allow sightings to be made on the actual star instead of the simulated star at the celestial pole. The outermost annulus of the 8 in diameter collimated beam is intercepted before it reaches the inclined mirror by a horizontal mirror on the inner support column, which stops the beam down to 6 in aperture and provides a reflected signal within the instrument for use in occasional checks of stability and alignment. When not in use the ring mirror is tilted out of the way through an angle of about a degree by means of a cam operated by an external lever working through a rotary vacuum seal. The ring mirror can be removed entirely, if desired, to restore the full 8 in diameter collimated beam through the exit window.

The substrates for all mirrors are fused silica; all transmitting optics (windows, wedges, tipping plates, etc.) are BSC-s or BK-7 optical crown glass of Schlieren quality, except for lenses in the eyepiece assembly. The total reflecting optical coatings are evaporated aluminum with silicon dioxide overcoating. The overall quality of the transmitted parallel beam out of the exit pupil of the collimator is better than one-tenth wavelength.

The light source is a small 2W "grain of wheat" tungsten filament lamp with an appropriate condenser lens to focus the filament on to the pinhole which is inside the vacuum chamber. The pinhole is attached to the inner support tube. An eyepiece is provided to allow the collimator to be used as a telescope to look into the star-tracker or other components counted in the dewar. The eyepiece also enables the instrument to be converted into a manual autocollimator when a mirror is placed in the exit beam. For ease of use the eyepiece is extended apporximately 24 in up from the pinhole assembly. Both the eyepiece and light source are supported from a common frame attached to the outer vacuum tube rather than the inner support column. They are thus isolated from the pinhole as well as the rest of the optics, so that the collimator is not disturbed when either is touched.

The pinhole size and calibration have already been discussed. To keep watch on short term variations in light intensity a phototube is incorporated in the same structure as the eyepiece and tungsten lamp. It receives light reflected via a mirror from the edge of the diverging bundle before the beam enters the pinhole, and the output signal is recorded along with the outputs from the experiment.

In addition to the levelling and tangent screws for mechanical alignment there are numerous optical adjustments. Focusing is accomplished by sliding the pinhole reticle tube in its holder on the support tube. The two folding mirrors in the diverging beam are each supported by aluminum buttons, which were coined down during assembly until the alignment was correct. The off-axis parabola is adjusted with three fine pitch screws against the edge of its figured surface. The mirror is held against these locating points by spring detents opposite each screw. Neither the off-axis parabola nor the folding mirrors are likely to need readjustment. The parallel beam deflecting mirror is mounted on a swinging bracket as already described, and is adjusted in its cell by two screws bearing on the edge of the mirror surface which align the mirror in azimuth. The entire cell is tilted to provide latitude adjustment.

Further fine adjustments in the direction of the main beam are accomplished by means of two tipping plates in the diverging bundle, one of which moves the beam in azimuth and the other in elevation. The range of motion is ±50 arc-s for each,and each is independent of the other. The dial reads from zero to 100 and a counter counts up to ten revolutions. There is a numbered division for each second of arc and ten line divisions between each

numbered line. Thus the dial reads from zero to 100 arc-s with 0.1 arc-s per division, with easy interpolation to 0.01 arc-s. The tipping plate is a plane parallel block of Schlieren quality crown glass, 1/2 in thick. It is mounted on flexure pivots to avoid lubrication problems in the vacuum and is moved by a lever working through a bellows to monitor a vacuum seal without friction or "stiction".

The tipping plates provide the adjustment for centering the star image on the roof prisms of the quartz telescope. There are in addition two motor-driven "dither plates", about 10 mils thick, also in the diverging bundle, which may be used to make the beam oscillate back and forth through 0.01 arc-s at frequencies up to 30 Hz. The plates are each driven with a cam on the shaft of a four pole synchronous motor; the rate of dither is determined by the frequency of the 110 volt a.c. power delivered to the motor. One dither plate oscillates the beam in aximuth and the other in elevation; they are independent and may be driven at the same time. Like the tipping plates they are mounted on flexure pivots and worked through bellows connections into the vacuum.

The combination of tipping and dither plates allows for thorough exploration of the star image. The tipping plates locate the image in any desired position in the field; the dither plates make the image oscillate about that position with known amplitude and frequency in either axis. Thus measurements of both the intensity of the signal and the magnitude of its first derivative can be made throughout the field, and from these the linearity of the star-tracker can be determined.

To convert the instrument into a two axis automatic autocollimator there is an autocollimating attachment which replaces the eyepiece/pinhole assembly. Details of the design and use of this attachment, and of a biaxial tiltmeter which can be mounted on the inner support tube to detect tilting motions of the star/collimator unit, are given elsewhere.[31] The instrument was designed by D.E. Davidson; most of parts were fabricated by D.A. Davidson; assembly and initial alignment of the optics was performed at Stanford in October 1975 by D.E. Davidson.

As remarked earlier the calibrated artificial star by reference to measurements at Lick observatory with the stellar photometer, concentrating our observations on Arcturus and Vega, both of which were high in the sky. We thank D.E. Osterbruck, Director of Lick Observatory, for permission to use the Crossley reflector, and G. Harlan for help in setting up our instrument.

Telescope performance

After calibrating the artificial star we mounted the telescope in its cradle, fabricated the light guides between the telescope and chopper assemblies, and transferred the chopper assemblies and new telescope electronics from the old star simulator where they had been under test. The first light guides were rigid coherent fiber optic pipes which had to be formed exactly to shape; later we replaced these with flexible incoherent light guides.

The first measurements using the original rigid light pipes provided useful experience but gave a noise performance of 20 marc-s in a 0.3 Hz bandwidth, barely as good as the results of Figure 7 and well short of our design goal. One peculiarity was a discrepancy of a factor of three between the noise levels in the two channels. The difference was traced to differences in noise performance of the two RCA 4441A photomultiplier, though these had been matched six years earlier to 10%. Differential aging of this order in photomultipliers over long periods is not unusual, and is reflected in our demand for an automatic gain control in the telescope readout, though that of course compensates for variations in scale factor not noise performance. The sensitivity of the better detector in these early measurements was 0.67 V/arc-s.

In the set up as first used there were still difficulties with the transmission of light from the telescope to the photodetector. Dr. Siddall improved matters by replacing the rigid light pipes with flexible non-coherent ones and devising a better clamping method to allow adjustment of the light pipes to their optimal positions at each end. The sensitivity in the more sensitive channel increased to 2.2 V/arc-s. Other improvements were made to the alignments of the telescope and artificial star, to definition of the star image (by using a smaller pinhole) and to the method of taking the data, particularly in treating the noise. J.T. Anderson and R.R. Clappier aided in the latter work. Much of the noise proved to be not intrinsic to the telescope. Vibrations in the building due to seismic noise and an air conditioner tended to excite the artificial star structure at its natural frequency of 13.2Hz,affecting the noise measurements and making static measurements of telescope linearity in the marc-s range exceedingly difficult. It was partly in anticipation of such difficulties that we installed the motor driven dither plates in the star/collimator unit to allow dynamic calibration methods.

Figure 9 shows the noise measurements presented in the form of a power spectral density

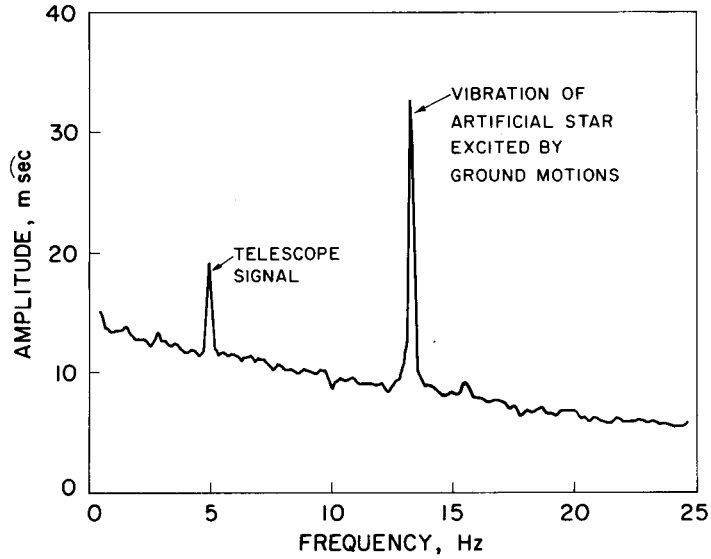

Figure 9: power spectral density of measured telescope noise

curve, with an oscillatory motion of amplitude 10 marc-s and frequency 5 Hz being injected into the apparent position of the star by means of the dither plates. The 13.2 Hz signal from the vibration of the star/collimator is clearly visible with an amplitude of about 25 marc-s. The filter-cut off used in most of the measurements was 5 Hz. At that frequency the noise observed had fluctuations but a long term average amplitude less than 10 marc-s. Translated to 1 Hz this corresponds to a noise performance of 4 marc-s as compared with the 1 marc-s that is the ultimate theoretical limit for diffraction limited optics applied to a point star.

Figure 10 shows results of linearity measurements. The measurement is not at present sufficiently precise to be of any use in checking the telescope linearity down to or below a marc-s. It shows, however, that the star image is of considerable larger diameter than

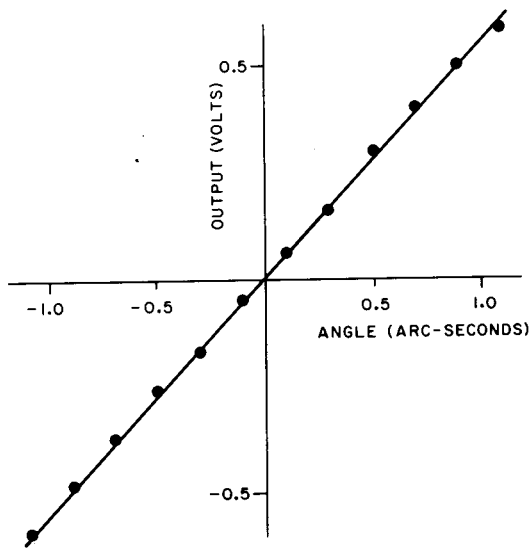

Figure 10: preliminary measurements of telescope linearity

would be expected from an 0.94 arc-s Airy disk; other measurements make the diameter to be more like 6 arc-s. Part of this anomalously wide range can be accounted for by the finite diameter of the pinhole in the artificial star, but not all. We conjecture that when these measurements were taken either the telescope or artificial star was out of focus. Since the system has been dismantled in preparation for transfer to a new location we have no method at present of determining which.

Taken together the results of Figure 9 and 10 give us grounds for encouragement about the telescope performance. Since, as Figure 10 indicates, the image was in effect defocused to a diameter several times that of the Airy disk we would expect noise level modestly higher than that from the ideal photon noise limit for a focused image (1 marc-s/$Hz^{\frac{1}{2}}$). The observed level of 4 marc-s/$Hz^{\frac{1}{2}}$ appears very reasonable. We plan to resume telescope testing within the next year.

Acknowledgements

This work was supported by NASA Grant NsG-582 (later NGR05-020-019) and NASA Contract NAS8-25705.

In addition to the many colleagues mentioned expliatly in the text we thank W.M. Fairbank for his constant enthusiastic interest; D.B. DeBra for many discussions, especially of the control issues; R. Decher and R.A. Potter of NASA Marshall Center for aid and guidance during the telescope development; G.M. Hunt and C. Jones also of NASA Marshall Center for contributing to the vibration tests; and H. Gey of Davidson Optronics for aid in the noise and linearity measurements with the telescope simulator.

References

1. Bardas, D., Cheung, W.S., Gill, D., Hacker, R., Keiser, G.M., Lipa, J.A., Macgirvin, M., Saldinger, T., Turneaure, J.P., Wooding, M.S.: "Hardware Development for Gravity Probe-B", SPIE Proceedings, Vol.619, 1986.

2. Everitt, C.W.F.: "The Stanford Relativity Gyroscope Experiment: History and Overview" in Near Zero: New Frontiers of Physics - Papers in Honor of William M. Fairbank, (ed., Deaver, B.S., Everitt, C.W.F., Fairbank, J., Michelson, P.M., New York, Freeman, W.H.), 1986.

3. Young, L.S.: "Systems Engineering for the GP-B Program", SPIE Proceedings, Vol.619, 1986.

4. Anderson, J.T. and Everitt, C.W.F.: "Limits on the Measurement of Proper Motion and the Implications for the Relativity Gyroscope Experiment", W.W. Hansen Laboratories of Physics, Stanford University, 1979, (unpublished report).

5. Pugh, G.E.: WSEG Research Memorandum No.11, Weapons System Evaluation Group, The Pentagon, Washington 25, D.C., 1959.

6. Frisch, D.H. and Kasper, J.F., Jr.: "Autometric Gyro for Satellite Relativity Experiments", Journal of Applied Physics, Vol.40, No.8, pp.3376-3381, 1969.

7. Fairbank, W.M. and Everitt, C.W.F.(Principal Investigators):"Final Report on Contract NAS8-25705 to Build and Test a Precision Star-Tracking Telescope", W.W. Hansen Laboratories of Physics, Stanford University, p.1, 1972.

8. Reference (7), pp.17-18.

9. Reference (7), pp.19-20.

10. Lange, B.O.: "Development of the Precision Stellar Monitor" in D.B. DeBra (Coordinating Principal Investigator) Final Engineering Report on a Continuing Program of Advanced Research in Guidance, Control and Instrumentation, Guidance and Control Laboratory, Stanford University, pp.25-30, 1970.

11. Van Patten, R.A., DiEsposti, R., Breakwell, J.V.: "Ultra High Resolution Science Data Extraction for the Gravity Probe-B Gyro and Telescope", SPIE Proceedings, Vol.619, 1986.

12. Everitt, C.W.F. (ed.): Report on a Program to Develop a Gyro Test of General Relativity in a Satellite and Associated Control Technology, W.W. Hansen Laboratories of Physics, Stanford University, p.334, 1980.

13. We thank R.B. Emmons and R. Vassar for pointing out an error in our earlier calculations of the numerical coefficient of the third term in the brackets.

14. Emmons, R.B.: Lockheed Report LMSC-F066052A EM-004 Appendix A.

15. Grossman, S.B. and Emmons, R.B.: "Performance Analysis and Size Optimization of Focal Planes for Point Source Tracking Algorithm Applications", Optical Engineering, Vol.23, No.2, pp.167-176, 1984.

16. Emmons, R.B. and Grossman, S.B.: "Telescope Noise Analysis", Lockheed Report LMSC-F066052A EM-004.

17. Nidey, R.A.: Memorandum to C.W.F. Everitt, dated October 21, 1968.

18. Parmley, R.T., Goodman, J., Regelbrugge, M., Yuan, S.: "Gravity Probe B Dewar/Probe Concept", SPIE Proceedings, Vol.619, 1986.

19. Woodruff, R.: Private communication in 1971. This work was done as part of the response to NASA Contract NASW-2284, summarized in Ball Brothers Research Corporation, "Mission Definition Study for the Stanford Relativity Satellite" (BBRC Report F71-07, December, 1971), which contains other valuable studies on the design of the telescope.

20. Sigler, R.: Gravity Probe-B Shuttle Test of Relativity Experiment, LMSC-D088466, Technical Appendix 1, p.1-2, 1984.

21. Angele, W., private communication.

22. It was already well known in 1876 when Maxwell referred to it in his lecture on "Action at a Distance", Scientific Papers, Vol.2, p.314, Cambridge, 1890. Note in reading this passage that Maxwell's terminology is different from contemporary usage.
23. Lord Rayleigh: "A Study of Glass Surfaces in Optical Contact", Proceedings of Royal Society, Series A, Vol.156, pp.326-349, 1936.
24. Wright, J.J. and Zissa, D.E.:"Optical Contacting for Gravity Probe Star Tracker", NASA Technical Memorandum NASA TM-86475, 1984.
25. Berthold, J.W., Jr., Jacobs, S.F., Norton, M.A.: "Dimensional Stability of Fused Silica, Invar, and Several Ultra Low Thermal Expansion Material", Applied Optics, Vol.15, No.8, p.1898, 1976.
26. Payne, L.L.: "Optical Contacting of Quartz", report submitted as part of NASA-ASEE Summer Faculty Research Fellowship Program, coordinated by University of Alabama in Huntsville through contract with Marshall Center, 1982.
27. Barber, T.D.: "A Theoretical Study of Optical Contact of Vitreous Silica." NASA Contract Report No. CR-61385, 1972.
28. Ghita, C. and Ghita, L.: "Hardening of Quartz Optical Contact by Thermal Treatment", Review of Scientific Instruments, Vol.43, No.7, p.1051, 1972.
29. But see also the discussion in Reference (24) pp.6-7.
30. Fairbank, W.M. and Everitt, C.W.F.: Final Report on Contract NAS8-25705 to Build and Test a Precision Star-Tracking Telescope", W.W. Hansen Laboratories of Physics, Stanford University, p.41 and Figures 11, 12, 1972.
31. Everitt, C.W.F. (ed.): Report on a Program to Develop a Gyro Test of General Relativity in a Satellite and Associated Control Technology, W.W. Hansen Laboratories of Physics, Stanford University, p.359, 1980.